

# Bypass of DNA interstrand crosslinks by a Rev1–DNA polymerase $\zeta$ complex

Rachel Bezalel-Buch<sup>1</sup>, Young K. Cheun<sup>2</sup>, Upasana Roy<sup>3,4</sup>, Orlando D. Schärer<sup>2,5</sup> and Peter M. Burgers<sup>1,\*</sup>

<sup>1</sup>Department of Biochemistry and Molecular Biophysics, Washington University School of Medicine, Saint Louis, MO, USA, <sup>2</sup>Center for Genomic Integrity, Institute for Basic Science, Ulsan 44919, Republic of Korea, <sup>3</sup>Department of Chemistry, Stony Brook University, Stony Brook, NY 11794, USA, <sup>4</sup>Department of Biochemistry & Molecular Biophysics, Columbia University, New York, NY 10032, USA and <sup>5</sup>Department of Biological Sciences, School of Life Sciences, Ulsan National Institute of Science and Technology, Ulsan 44919, Republic of Korea

Received April 26, 2020; Revised June 18, 2020; Editorial Decision June 24, 2020; Accepted June 24, 2020

## ABSTRACT

**DNA polymerase  $\zeta$  (Pol  $\zeta$ ) and Rev1 are essential for the repair of DNA interstrand crosslink (ICL) damage. We have used yeast DNA polymerases  $\eta$ ,  $\zeta$  and Rev1 to study translesion synthesis (TLS) past a nitrogen mustard-based interstrand crosslink (ICL) with an 8-atom linker between the crosslinked bases. The Rev1–Pol  $\zeta$  complex was most efficient in complete bypass synthesis, by 2–3 fold, compared to Pol  $\zeta$  alone or Pol  $\eta$ . Rev1 protein, but not its catalytic activity, was required for efficient TLS. A dCMP residue was faithfully inserted across the ICL-G by Pol  $\eta$ , Pol  $\zeta$ , and Rev1–Pol  $\zeta$ . Rev1–Pol  $\zeta$ , and particularly Pol  $\zeta$  alone showed a tendency to stall before the ICL, whereas Pol  $\eta$  stalled just after insertion across the ICL. The stalling of Pol  $\eta$  directly past the ICL is attributed to its autoinhibitory activity, caused by elongation of the short ICL-unhooked oligonucleotide (a six-mer in our study) by Pol  $\eta$  providing a barrier to further elongation of the correct primer. No stalling by Rev1–Pol  $\zeta$  directly past the ICL was observed, suggesting that the proposed function of Pol  $\zeta$  as an extender DNA polymerase is also required for ICL repair.**

## INTRODUCTION

DNA Polymerase  $\zeta$  (Pol  $\zeta$ ) is a B-family DNA polymerase, which is involved in translesion DNA synthesis (TLS) (1). Unlike the other B family members (Pol  $\alpha$ , Pol  $\delta$ , Pol  $\epsilon$ ), which show a high replication fidelity, Pol  $\zeta$  has a low fidelity (2,3). Pol  $\zeta$  is a multi-subunit enzyme (Rev3, Rev7, Pol31, Pol32), sharing the Pol31 and Pol32 subunits with Pol  $\delta$  (4,5). While the Rev3:Pol31:Pol32 stoichiometry is ap-

proximately 1:1:1, that of Rev7 is substantially higher (5,6). However, the exact stoichiometry of Rev7 remains to be determined. Human Rev7 exists as a dimer (7), and furthermore, the human Rev3 subunit has two independent Rev7 binding sites (8). The interaction of Pol  $\zeta$  with the replication clamp PCNA increases its activity, presumably by increasing the processivity of the enzyme (5,9). Rev1 is a Y family DNA polymerase with a unique dCMP transferase activity (10). However, while *Saccharomyces cerevisiae* REV1 is absolutely required for damage-induced mutagenesis (11), its catalytic activity is not (12), suggesting that the non-catalytic functions of Rev1 are important. Therefore, Rev1 is considered mainly as a scaffold protein onto which the mutasome is assembled. It promotes mutagenesis by essential interactions with other factors, including mono-ubiquitinated PCNA and Pol  $\zeta$  (13–16), and in mammalian cells, also Pol  $\eta$  (17).

Cells deficient for Pol  $\zeta$  or Rev1 are sensitive to DNA damage and are among the most hypersensitive to treatment with interstrand cross-linking (ICL) agents, suggesting that they have a key role in ICL repair (18–23). DNA ICLs covalently link two strands of the double helix, thereby providing a complete block to both the DNA replication and the transcription machineries. ICLs can be formed by endogenous sources as well by antitumor agents such as nitrogen mustard and cisplatin (24,25). The removal of ICLs from genomes necessarily requires a complex repair process. Several pathways for ICL repair have been described. Although ICL repair also occurs in the G1 phase of the cell cycle, the removal of ICLs is most critical during S-phase, where they provide an absolute block to replication (26). ICLs can be encountered by the collision of two replication forks (27), or a unidirectional fork can traverse the ICL in a FancM-dependent step followed by priming and fork resumption downstream of the ICL (28). Regardless, all ICL repair pathways require an unhooking step to separate the two

\*To whom correspondence should be addressed. Tel: +1 314 362 3772; Fax: +1 314 362 7183; Email: burgers@biochem.wustl.edu

crosslinked strands and a DNA synthesis step to restore the duplex. Studies of the repair of site-specific plasmid-based ICLs in *Xenopus* egg extracts have provided a biochemical framework for understanding ICL repair and illustrate what roles DNA polymerases play in ICL repair (27). Activation of the Fanconi anemia (FA) pathway at the ICL leads to the recruitment of the ERCC1-XPF and possibly other endonucleases to unhook the crosslink from one of the two strands (29,30). The unhooked ICL may be trimmed further by an exonuclease such as SNM1A/Pso2 (31). The unhooked and processed ICL is then bypassed by translesion synthesis (TLS) DNA polymerases to generate one continuous duplex that can be used as a template to fix the second strand (27). While this FA-dependent pathway can act on most ICLs, several variants of this general pathway exist for ICLs formed by psoralen, abasic sites or acetaldehydes (32,33). Studies in the *xenopus* system showed that depletion of Rev1 from the extract inhibited the insertion step at the ICL site for cisplatin, but not acetaldehyde-induced ICLs, while it had an effect on the extension reaction for both lesions (16,33). Thus, depending on the ICL type, Rev1 may also be required for the insertion step. Furthermore, depletion of the Rev7 subunit of Pol  $\zeta$  inhibited the extension of the repair product past the insertion opposite a cisplatin ICL, in agreement with the known role of Pol  $\zeta$  as an extender polymerase (27). Biochemical studies have shown that various TLS polymerases can bypass ICLs (25,34–36), but conclusive studies of the bypass activity of purified Pol  $\zeta$  and Rev1 are missing. In this paper, we provide critical new information regarding the functions of Pol  $\zeta$  and Rev1 on an ICL substrate that mimics an unhooked nitrogen mustard lesion (34,37). Our studies show that Rev1 stimulates ICL bypass by Pol  $\zeta$ , but its enzymatic activity is largely dispensable. Both Pol  $\eta$  and Rev1–Pol  $\zeta$ , but not Pol  $\delta$  can mediate ICL bypass. However, Pol  $\eta$  shows very strong stalling directly past insertion at the ICL. In contrast, Rev1–Pol  $\zeta$  proceeds more efficiently past the ICL, suggesting that the enzyme is suitable for complete TLS.

## MATERIALS AND METHODS

### Reagents and enzymes

Chemical reagents were purchased from Sigma-Aldrich (St. Louis, MO, USA). USER™ Mix, T4 polynucleotide kinase, and T4 DNA ligase were purchased from New England Biolabs (Ipswich, MA, USA).

### Oligonucleotides and primers

The sequences of the oligonucleotides were listed in Supplementary Table S1. HPLC-purified fluorescent labeled primers, biotinylated extension oligonucleotides, and splint oligonucleotides were purchased from Integrated DNA Technologies (Coralville, IA, USA). Single-stranded oligonucleotides with ICL precursors, 39mer 20-bp ICL that contains two flanking uracil bases around the crosslinked base (39+20(6)-ICL), and 39mer 6-bp ICL (39+6-ICL) were synthesized and purified as previously reported (37). The identity of the ICLs was confirmed by LC-MS (Supplementary Figure S1A).

### Preparation of 93mer 6-bp ICL substrate (93+6-ICL)

39+6-ICL (500 pmol) was annealed with extension oligonucleotides (5'ext, 3'ext) and splint oligonucleotides (5'splint, 3'splint) in 1:1.2:2 ratio at room temperature overnight and reacted with T4 polynucleotide kinase (T4 PNK, 60 U) and T4 DNA ligase (4800 U) at 37°C for 1 h in the presence of 50 mM Tris–HCl (pH 7.5), 10 mM MgCl<sub>2</sub>, 1 mM ATP, 10 mM DTT. This procedure also removed the 3'-phosphate from the covalently attached hexanucleotide, due to the 3'-phosphatase activity of T4 PNK. The product of the ligation reaction was purified by 10% denaturing polyacrylamide gel electrophoresis containing 7 M urea. The desired band was visualized by UV shadowing, excised and the DNA extracted by electroelution (Schleicher & Schuell BT 1000 or Bio-Rad Model 422). The extracted DNA was desalted by centrifugal filtration (Merck Millipore Amicon Ultra-0.5 ml), and freeze-dried. The purified product was analyzed by 10% denaturing polyacrylamide gel containing 7 M urea and 1× TBE (Supplementary Figure S1B). A control substrate, which retained the 3'-phosphate on the hexanucleotide, was synthesized similarly (Supplementary Figure S6). In brief, 39+20(6)-ICL was 5'-phosphorylated by T4 PNK prior to USER digestion. The subsequent ligation of USER-digested ICL without the use of T4 PNK afforded 93 nt 6-bp ICL with 3'-phosphate block (93+6p-ICL).

### Preparation of 93mer 20-bp ICL substrate (93+20-ICL)

A 93 nt-long single-stranded DNA that contains an ICL precursor (T93-C2) was prepared by ligating T39-C2 to 5'ext and 3'ext. The reaction and the purification methods were identical to those of 93+6-ICL. The use of T39-G instead of T39-C2 gave the control undamaged 93mer substrate. An ICL was formed between T93-C2 and C20-C2 as previously (38). In brief, the two complementary oligonucleotides were annealed together, and then the ICL precursors were unmasked by sodium periodate to expose the aldehydes. The subsequent crosslink reaction by *N,N'*-dimethylethylenediamine in the presence of sodium cyanoborohydride at pH 5.4 effected the formation of the eight atom ICL between T93-C2 and C20-C2. The purification method was identical to that 93+6-ICL. The purified product was analyzed by 10% denaturing polyacrylamide gel containing 7 M urea and 1X TBE (Supplementary Figure S1B).

### Proteins

All proteins are the *S. cerevisiae* species and were purified as previously described. Pol  $\zeta$ , Rev1–Pol  $\zeta$ , Rev1 and Rev1 mutants, Pol  $\eta$ , Pol  $\delta$  and Pol  $\delta$ -DV (D520V) were purified from yeast overexpression systems (5,6,9,39). RPA, PCNA and RFC were purified from *Escherichia coli* overexpression systems (40–42).

### DNA polymerase assay

The 10  $\mu$ l assay contained 40 mM Tris–HCl pH 7.8, 1 mM DTT, 0.2 mg/ml bovine serum albumin, 8 mM Mg-acetate, 100 mM NaCl final (this includes all contributions from the

added enzymes), 0.5 mM ATP, DNA damage-response concentrations of dNTPs (6): 195  $\mu$ M dCTP, 383  $\mu$ M dTTP, 194  $\mu$ M dATP and 50  $\mu$ M dGTP, 10 nM control or ICL DNA substrate, 40 nM RPA, 30 nM PCNA and 10 nM RFC. PCNA was loaded by RFC for 30 s at 30°C, and reactions were initiated with 25 nM of DNA polymerase. Assays containing the (mutant) Rev1–Pol  $\zeta$  complex were initiated with 25 nM Pol  $\zeta$  and 75 nM Rev1, which were preincubated on ice for 10 min or more. Aliquots were stopped with an equal volume of PK stop solution (20 mM EDTA, 1% SDS, 0.8 mg/ml Proteinase K), and incubated at 50°C for 30 min, followed by precipitation with an equal volume of 2.5 M  $\text{NH}_4$ -acetate, 0.1 mg/ml glycogen. Then, 2.1 volumes of cold ethanol were added and, after cooling at –20°C for 30 min, the DNA was collected at 17 000  $\times$  g in a refrigerated centrifuge for 20 min, followed by a 70% ethanol wash. The dried DNA pellet was re-suspended in 10  $\mu$ l of 10 mM Tris–HCl pH 7.5, 1 mM EDTA, 50 mM NaCl, 0.2% SDS and incubated at 50°C for 1 h. An equal volume of sequencing solution was added to a final concentration of 50% formamide and 10 mM EDTA, and the samples were analyzed on 12% polyacrylamide-7 M urea gels. Detection was carried out with a Typhoon phosphorimager in the fluorescence mode, and the data were quantified with ImageQuant (GE Healthcare), or with ImageJ software (after conversion of the Typhoon data by linearization). KaleidaGraph software was used for plotting. Note that the FAM-primers show variable ghosting of fluorescence at positions ~1–2 nt higher. These ghosting phenomena are only for unreplicated primers and disappears upon replication.

### Polymerase exchange during TLS

The polymerase exchange assay was as the TLS assay, with modifications. The assay mixture contained 100  $\mu$ M AMP–CPP instead of ATP for PCNA loading by RFC (the  $\alpha$ – $\beta$ -methylene group allows proficient loading of PCNA but not replication by DNA polymerases when dNTPs are omitted) (43). Subsequently, DNA polymerase(s) were added to the assay, and, after 30 s, replication was initiated by addition of dNTPs. Reactions were terminated after 15 min and processed as described above.

### Sequencing of the TLS synthesis products

Reactions were increased to 50  $\mu$ l and allowed to proceed for 60 min, stopped with final concentration of 50% formamide, 10 mM EDTA and 0.1% SDS, and loaded on a 12% polyacrylamide-7 M urea preparative gel. Full-length products were extracted from the gel and purified by the ZR small RNA PAGE recovery kit (Zymo Research – R1070). Sequencing primer 5'-AAGCTGGAGCTCCACCGCGG-3' was annealed and sequencing was performed with the USB Sequenase Version 2.0 DNA sequencing kit (Thermo Fisher Scientific – 70770).

## RESULTS

### Generation of ICL substrates for PCNA-mediated polymerase bypass

We and others have previously shown that the structure of the ICL that links two bases as well as the length of the du-

plex around an ICL affects bypass by DNA polymerases (34,35,37). We used our previously published method to generate a stable nitrogen mustard ICL mimic with an 8 atom crosslink through a double reductive amination reaction of an aldehyde ICL precursor with dimethylethylenediamine embedded in a 6mer duplex (8a-6 bp ICL, Figure 1A) (38,44). Our design was based on the consideration that (i) when replication forks stall, ~20 nucleotides remain unreplicated between the leading strand 3'-end and the ICL, and (ii) that nucleolytic processing of the non-template strand leaves the unhooked ICL in a duplex of only a few nucleotides (27). To the initially obtained ICL on a 39mer template, we ligated 5' and 3' biotinylated oligos to generate a 93mer substrates with biotinylated ends. This procedure also served to remove the 3'-phosphate on the covalently attached hexamer (Figure 1A). The biotin moieties at either template terminus were introduced to bind streptavidin to form blocks to prevent PCNA from sliding off the DNA (9). The control substrate (undamaged DNA) lacks the ICL and the six nucleotides of dsDNA, which would not form a stable duplex with the template strand in the absence of the ICL.

### In vitro bypass of an ICL by Pol $\eta$ and Rev1–Pol $\zeta$

We have previously shown that Pol  $\zeta$  can be purified as a stable multi-subunit complex together with Rev1 (6). A complex with the identical activity can also be obtained by simply mixing Pol  $\zeta$  together with Rev1. In this paper, we have reconstituted the various complexes of Rev1–Pol  $\zeta$  by mixing Rev1, or Rev1 mutants, together with wild-type Pol  $\zeta$ .

The DNA substrates were pre-incubated with the single-stranded DNA binding protein RPA (replication protein A), and PCNA (proliferating cell nuclear antigen) was loaded by RFC (replication factor C) and ATP, as shown in Figure 1B. The reaction was started by addition of the individual DNA polymerases. dNTPs were present at concentrations that prevail during the DNA damage response in yeast (6). Replication of the undamaged control DNA was carried out very efficiently, with the exception of replication by Rev1–Pol  $\zeta$  (lane 5, discussed below). The presence of the streptavidin moiety at the template 5'-end sterically limits full extension by Pol  $\delta$  (lanes 1,2) and Pol  $\zeta$  (lanes 4,5), compared to Pol  $\eta$  (lane 3), and this pattern was also displayed with the ICL-containing substrates.

Pol  $\delta$  stalled mainly at the nick position, four nucleotides prior to encountering the crosslinked G residue (Figure 1C, lanes 6–9), consistent with its known idling function at nicks, an iterative process of polymerase activity followed by 3'exonuclease activity (45). However, ~2–3% full-length product was observed at every time point, which could be due to incomplete crosslinking of the substrate or a low level of bypass by Pol  $\delta$  (see also Supplementary Figure S2A). This non-specific background observed by wild-type Pol  $\delta$  was subtracted from the percentage of extension products observed with the TLS enzymes. First, we eliminated the proofreading function of Pol  $\delta$  (Pol  $\delta$ -exo<sup>-</sup>, D520V). This eliminated idling at the nick (45), but still allowed only minimal bypass synthesis over the 30 min time-course of the assay (Figure 1C, lanes 10–13; Figure 1E).

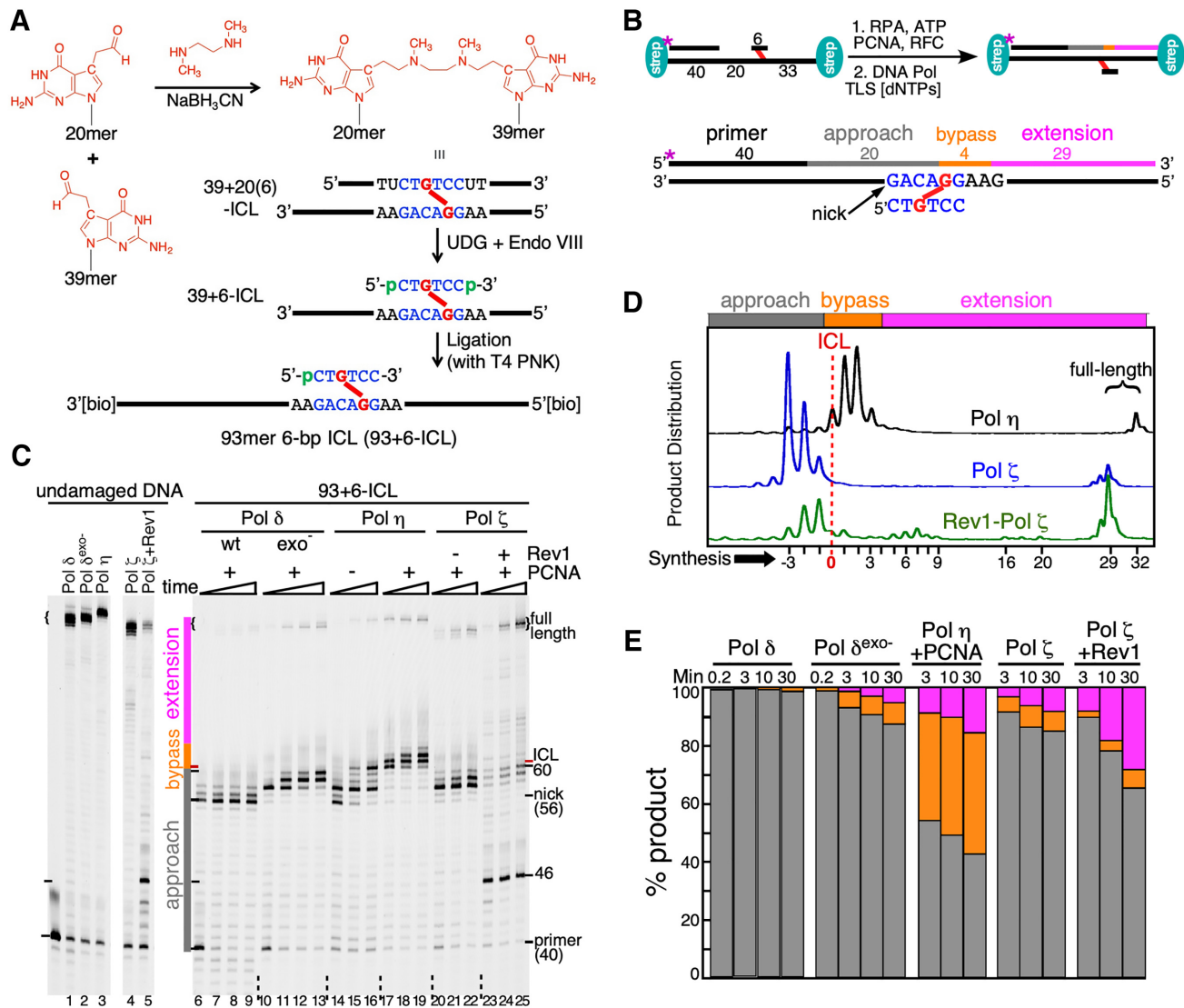


**Figure 1.** Translesion DNA synthesis of an ICL by yeast DNA polymerases. (A) Synthetic scheme for the 93mer 6-bp ICL substrate. UDG, uracil-DNA-glycosylase; Endo VIII, *E. endonuclease VIII*. See Materials and Methods for details. (B) Top, schematic overview of the DNA substrate and the assay set-up. \*, 5'-fluorescein (FAM) label. Strep, biotin-streptavidin block. This block at the template 5'-end forms a barrier, preventing the bulky Pol  $\delta$  and Pol  $\zeta$  enzymes from replicating the template up to the very end, while the small Pol  $\eta$  enzyme does proceed up to the end of the template (panel C). Bottom, designation of specific classes of elongation products: Approach, gray; Bypass, orange; Extension, pink. TLS [dNTPs] are concentrations that prevail under damage response conditions in yeast. See Materials and Methods for details. (C) Time course of replication of control DNA (lanes 1–5) or ICL DNA by the indicated DNA polymerase, with or without PCNA for Pol  $\eta$ , and with or without Rev1 for Pol  $\zeta$ . The gel was cut up for easier visualization (the entire gel is shown in Supplementary Figure S2A). (D) The extension products, from a 53-mer size up to full-length, obtained by scanning lanes 19, 22 and 25, were plotted. The presence of the streptavidin block at the template 5'-end limits full replication by the bulky Pol  $\zeta$  and Rev1–Pol  $\zeta$  enzymes, compared to Pol  $\eta$ . (E) Quantification of the replication products from (C) into three classes.

Based on previous studies of TLS by Pol  $\eta$ , we have divided the replication products into three classes for the purpose of quantification (37). Products up to the ICL are designated as ‘**approach**’, those that have inserted a nucleotide opposite the crosslinked G, plus an additional three nucleotides past the ICL are designated as ‘**bypass**’, and those longer than that up to full-length are designated as ‘**extension**’. Quantification is shown in Figure 1E. The bypass of this particular ICL has been studied previously, however these model studies were carried out with Pol  $\eta$  alone, without the PCNA clamp and at low salt concentrations (37). TLS by Pol  $\eta$  alone was most efficient at low salt (50 mM

NaCl, Supplementary Figure S2B). For sake of consistency, all studies in this paper were carried out at 100 mM NaCl. Under these conditions, the limited bypass of the ICL by Pol  $\eta$  was stimulated substantially by PCNA (Figure 1C, compare lanes 14–16 with 17–19 and Supplementary Figure S2B, compare lanes 7–9 with 10–12, and 13–15 with 16–18). However, as observed previously (37), the majority of products are still stalled at the +1 to +3 positions. Notably, the % of bypass and extension showed very little time dependence. After 30 min incubation, bypass had increased only 1.2-fold compare to the 3 min incubation, and extension only 1.5-fold (Figure 1E). In contrast to Pol

$\eta$ , Pol  $\zeta$  stalled predominantly prior to the ICL, similar to proofreading-defective Pol  $\delta$  (lanes 20–22). However, significant bypass and extension was observed by Pol  $\zeta$ , although less efficiently than by Pol  $\eta$ . Notably, the lack of products at the +1 to +3 positions, together with the presence of fully replicated DNA indicates that, once a nucleotide has been inserted opposite the ICL-G position, this product is favorably accommodated in the Pol  $\zeta$  binding site to allow continued extension. This remarkable difference between Pol  $\eta$  and Pol  $\zeta$  is shown graphically in Figure 1D.

Three dramatic changes were observed with Rev1–Pol  $\zeta$  as TLS enzyme compared to Pol  $\zeta$  alone. First, strong pause sites were observed during replication of normal (undamaged) DNA (Figure 1C, lanes 4 and 5). The inhibition of Pol  $\zeta$  activity by Rev1 on undamaged DNA is the subject of a different study (Bezalel-Buch, R. and Burgers, P. unpublished data). Replication of the ICL-DNA also shows these ICL-independent distant pause sites, in addition to ICL-dependent pause sites directly ahead of the crosslink. Second, synthesis past the ICL is enhanced by the inclusion of Rev1 (Figure 1C, lanes 23–25). Third, once bypass has been achieved, further replication of the downstream template is once more inhibited as is evident from the presence of multiple, distant stall sites. After 30 min, the total extension products by Rev1–Pol  $\zeta$  are about 30% compared to 10% with Pol  $\zeta$  alone (Figure 1C–E).

### The catalytically inactive form of Rev1 stimulates Pol $\zeta$ -mediated ICL bypass

The data in Figure 1 show clearly that Rev1 has an important role in Pol  $\zeta$ -mediated ICL bypass and extension. To assess whether this is due to the catalytic function of Rev1 or to its proposed scaffolding function, we repeated the TLS assay with Rev1<sup>cd</sup> (Rev1-DE467,468AA), a catalytic-inactive mutant of Rev1 (Figure 2A, (12)). Remarkably, the efficiency of ICL bypass and the extension by Rev1<sup>cd</sup>-Pol  $\zeta$  was higher than by Pol  $\zeta$  alone, and it is diminished only slightly from that observed with wild-type Rev1–Pol  $\zeta$  (Figure 2B). The major difference is the stronger accumulation of stalled products directly prior to the ICL, suggesting the participation of the catalytic activity of Rev1 at the ICL. Interestingly, the major lesion-independent stall site at position 46 is still present albeit reduced by 30–55% (Figure 2A, lane 3 versus 4, and lanes 11–13 versus 14–16). In addition, post-ICL stall sites are somewhat reduced, including a minor site at position 70. In order to determine the possible participation of the catalytic activity of Rev1, we sequenced the fully replicated products from a 60 min assay, which resulted in >60% full-length product accumulation (not shown) (Figure 2C, Supplementary Figure S3). Remarkably, while bypass of the major stall site at position 46 (across a dC template) is not associated with dCMP misincorporation (Supplementary Figure S3), bypass of the minor stall site at position 70 (across a dC template) is associated with misincorporation of dCMP with a 15–20% efficiency (three determinations). Misincorporation is carried out by Rev1's dCMP transferase activity, since it is not present with Pol  $\zeta$  alone, and eliminated with Rev1<sup>cd</sup>-Pol  $\zeta$  (Figure 2C). Therefore, the inhibitory mechanisms of Rev1 on non-damaged DNA involve both its catalytic

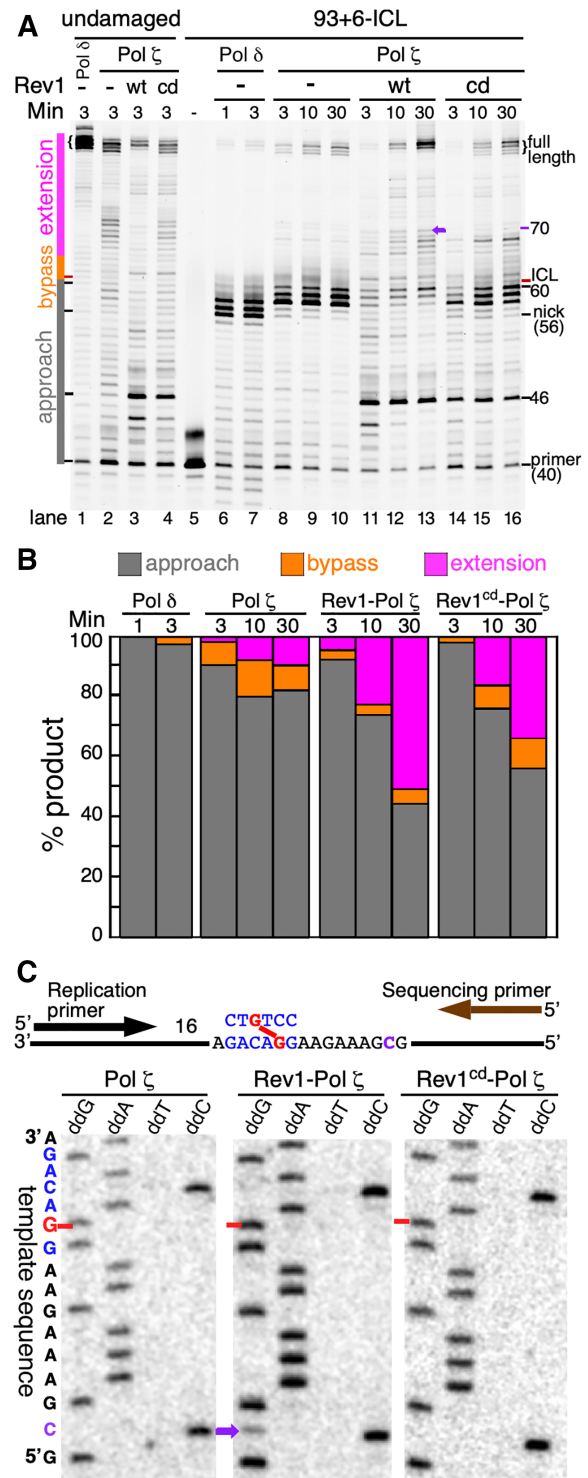


**Figure 2.** Catalytically inactive Rev1 stimulates ICL TLS by Pol  $\zeta$ . (A) Time course of replication of control DNA (lanes 1–4) or ICL DNA by the indicated DNA polymerase, with or without Rev1 for Pol  $\zeta$ . Rev1<sup>cd</sup> is catalytic-dead (D467A/E468A). (B) Quantification of the replication products into three classes. (C) ICL bypass product sequence analysis. Top, schematic map of the assay. Full-length replication products were isolated from 60 min assays. Bottom, sequencing analysis. The red arrow indicates the ICL-dG template position, which is replicated by insertion of dCMP, which is sequenced as a dG. The purple arrow, also shown in (A) at position 70, indicates a position where Rev1, but not Rev1<sup>cd</sup> misincorporates dCMP across from template dC with a frequency of 15–20%.

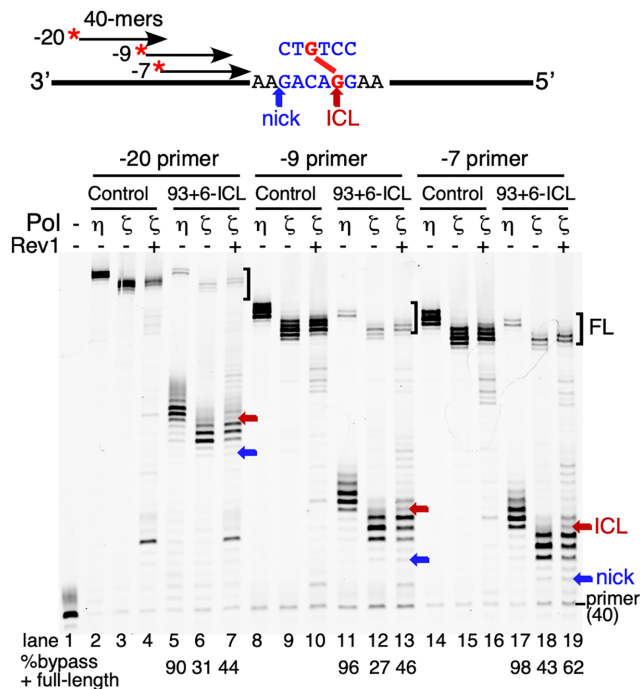


**Figure 3.** Primer distance from the ICL influences TLS efficiency. Top, schematic map of the three different 40-mer primers, the nick location and the ICL position. Bottom, gel analysis of the assays, with either the control or ICL substrates. Replication was carried out for 15 min with either Pol η, Pol ζ or Rev1–Pol ζ, as indicated. Blue and red arrows indicate nick and ICL positions, respectively, for the different substrates. At bottom, quantification of the % bypass + % extension products (see Figure 1B). FL, full length; see legend to Figure 1 for explanation of migration artifacts.

and scaffolding functions. Within the sensitivity of detection (>95%), all three enzymes (Pol ζ, Rev1–Pol ζ, Rev1<sup>cd</sup>–Pol ζ) faithfully introduced a dCMP across the ICL-G position (Figure 2C).

### Distance of the primer terminus from the ICL influences TLS by Rev1–Pol ζ

It is not entirely clear where and when during DNA replication and translesion synthesis, a TLS polymerase takes over DNA synthesis. Is it when replication stalls ~20 nt before the ICL (on the leading strand), or only when the ICL position is reached? A recent study in *Xenopus* egg extract suggests that the approach is carried out by a replicative DNA polymerase, up to one nucleotide before the ICL position, and bypass and extension is performed by a complex of Rev1 and Pol ζ (16). We determined the efficiency of ICL bypass as a function of the distance between the primer terminus and the ICL (Figure 3). The three primers were 40 nt in length and were positioned with their 3'-termini at either 20 nt, 9 nt or 7 nt from the ICL position. Pol η showed efficient bypass with all three substrates, and stalling at the +1 to +3 positions past the ICL remained unaffected. Bypass by Pol ζ alone was stimulated slightly when the primer was positioned closer to the ICL (compare lanes 6, 12 and 18). However, we noticed a significant improvement in bypass synthesis by Rev1–Pol ζ when the primer terminus position was closer to the ICL (compare lanes 7, 13 and 19).

To a large extent this increase in efficiency can be attributed to the elimination of the ICL-independent strong stall sites by hybridization of the closer primers. As expected, once the ICL was bypassed, Rev1–Pol ζ stalled similarly at downstream template positions. The distance between the primer terminus and the ICL did not affect the identity of the nucleotide incorporated opposite the ICL-G. With both the –20 and the –7 primer (with relation to the ICL), this was a dCMP residue, introduced either by Pol η, by Pol ζ or by Rev1–Pol ζ (Supplementary Figures S3 and S4). Note that by the nature of the assay, this analysis does not address what residue is inserted across the ICL by Pol η with regard to those products that are terminally stalled at the +1 to +3 positions.

### The interplay between different DNA polymerases in ICL bypass

While it is well recognized that Pol ζ and Rev1 are indispensable for the TLS of ICLs in eukaryotic cells, Pol η can contribute to the efficiency of this process (46). Switching between Pol η and other DNA polymerases has been observed with pyrimidine dimer lesions (47–49). Does switching also occur during the TLS of ICLs, and with what efficiency? This is of particular interest since Pol η stalls at positions past the ICL. One interpretation of this result is that bypass may be associated with misinsertion to yield mismatched primer termini, which could be dead-end products for further elongation by Pol η. However, such mismatched termini should provide good substrates for extension by Pol ζ or Rev1–Pol ζ, because this enzyme is an efficient extender of mismatches (3,50,51). Therefore, we investigated a potential collaboration between DNA polymerases in ICL bypass. In the assay we used all combinations of Pol δ, Pol η, Pol ζ and Rev1 (Figure 4A).

Lanes 2–5 represent the reactions with one DNA polymerase. These data recapitulate the data shown in Figure 1, with Pol δ stalling at the nick, Pol η at the 0 (ICL), +1 and +2 positions, Pol ζ 1–3 nucleotides before the ICL, and Rev1 alone stalling after incorporation of one single nucleotide. With the exception of Rev1–Pol ζ, the combination of two DNA polymerases did not increase bypass and extension significantly. In fact, the presence of Pol δ inhibited bypass by Pol η and Pol ζ (compare lanes 6, 7 with 3, 4). Surprisingly, Pol η plus Pol ζ did not yield a substantial increase in extension products compared to Pol η alone (compare lane 10 with 3). As shown earlier in this paper, only the Rev1–Pol ζ complex showed an increase in bypass and extension (lane 12). Next, three DNA polymerases were tested. Again, Pol δ showed only an inhibitory activity on bypass (lanes 13–15), by degrading extension products through its 3'-exonuclease activity as shown in Figure 1C. Surprisingly, like observed with the Pol η–Pol ζ couple, the combination of Pol η and Rev1–Pol ζ yielded only a marginal increase in bypass compared to Rev1–Pol ζ alone (compare lanes 16 and 12). Significantly, most products are stalled at the ICL and 1–2 nucleotides past the ICL, which is evidence of Pol η activity (lane 3). Finally, the four-polymerase bypass reaction again showed the inhibitory effect of Pol δ on TLS (lanes 16, 17).

We were surprised by the observation that the combination of Pol η and Rev1–Pol ζ did not give the anticipated

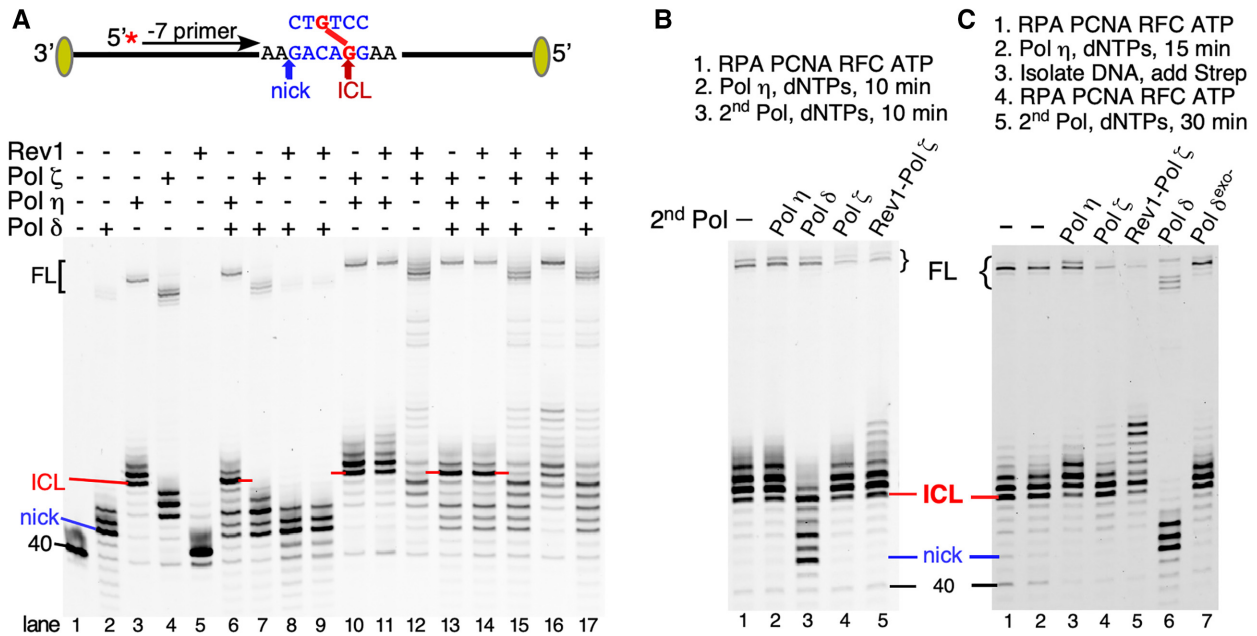


**Figure 4.** Polymerase exchange analysis in ICL bypass synthesis. The ICL substrate with the -7 primer was used. (A) Reactions were carried out for 15 min with either the individual DNA polymerases, or with a combination, which was added as a pre-formed mixture, as shown. Note that all lanes containing Pol δ show degradation products shorter than the 40 mer primer. These products were less than 10% of total. (B) Two-stage reaction with Pol η in the first 10 min incubation, followed by the indicated DNA polymerase in the second 10 min incubation. Lane 1, no second incubation; lane 2, incubation with Pol η continued. (C) Two stage ICL bypass assay. After the first incubation, the DNA was isolated (materials and methods), followed by second stage assay with the indicated DNA polymerase. Lane 1, product after first stage; lane 2, second stage incubation without added polymerase. FL, full length; see legend to Figure 1 for explanation of migration artifacts.

synergy in bypass. We had predicted that this combination would give excellent TLS because Pol η alone would produce mostly products that stalled past the ICL, while Pol ζ or Rev1–Pol ζ showed no stalling at these positions. Therefore, we expected that Pol ζ or Rev1–Pol ζ would readily extend the Pol η intermediates to full-length products (Figure 1D). However, this was not observed. We carried out a two-step bypass assay, in which the ICL substrate was replicated by Pol η in the first stage, and then further extended with other DNA polymerases in the second stage (Figure 4B). While Pol δ was inhibitory in the second stage, degrading the bypass products by Pol η (lane 3), Rev1–Pol ζ showed only minimal extension of the bypass products (lane 5).

We next examined the possibility that Pol η was bound up in a stalled, non-exchangeable (frozen) complex with the +1 to +3 bypass products, blocking access by Rev1–Pol ζ. This hypothesis needed testing, in spite of the observation that the 3'-exonuclease activity of Pol δ did have access to these stalled products (Figure 4B, lane 3). After the first stage, the DNA was reisolated by ethanol precipitation and subjected to the second stage assay (Figure 4C). Analogous results to those in Figure 4B were obtained. While Rev1–Pol ζ promoted significant propagation of the Pol η bypass products, it was still limited, yielding very few full-length products during the 30 minute incubation.

Translesion synthesis in the cell requires monoubiquitination of PCNA at Lys-164 (52). While monoubiquitinated PCNA (Ubi-PCNA) does not stimulate Pol ζ activity (13), it shows increased binding to Rev1 and it stimulates Rev1 activity in certain sequence contexts (13,15,53). Mutation of the ubiquitin-binding motif in

yeast Rev1 abolishes DNA damage-induced mutagenesis in yeast, supporting the model that Ubi-PCNA mediates its function through Rev1 (15). Studies with human Rev1, in which the ubiquitin-binding motifs were mutated, reached a similar conclusion (54). We carried out an experiment, in which PCNA and Ubi-PCNA were compared as accessory factor for TLS by multiple DNA polymerases, analogous to that in Figure 4A. However, we detected no significant difference in ICL bypass efficiency (Supplementary Figure S5). Our data are consistent with a model in which the main function of PCNA monoubiquitination is to recruit Rev1, and thereby Pol ζ to damaged chromatin for TLS. Interestingly, bypass by Pol η of abasic sites or UV damage is enhanced when PCNA is monoubiquitinated (13,55).

#### Autoinhibitory activity of Pol η during ICL bypass

We next investigated whether the bypass products made by Pol η were mere elongation products of the 40-mer primer, or whether other changes to the ICL substrate had occurred that were responsible to lead to an inhibition of the formation of full-length products. If primer elongation, for instance to the +2 position, were the only result of replicating the ICL substrate with Pol η, then that +2 product should be equivalent in activity to a substrate made by hybridizing the +2 primer to the ICL template. In the experiment in Figure 5, different length primers, with the same 5'-end but with their 3'-termini at the -7 position (the standard primer), at 0 (across the ICL), or at +2 or +6 position, were hybridized to the ICL template (Figure 5A). Their reactivities were assessed with each of the four enzymes. For the purpose of

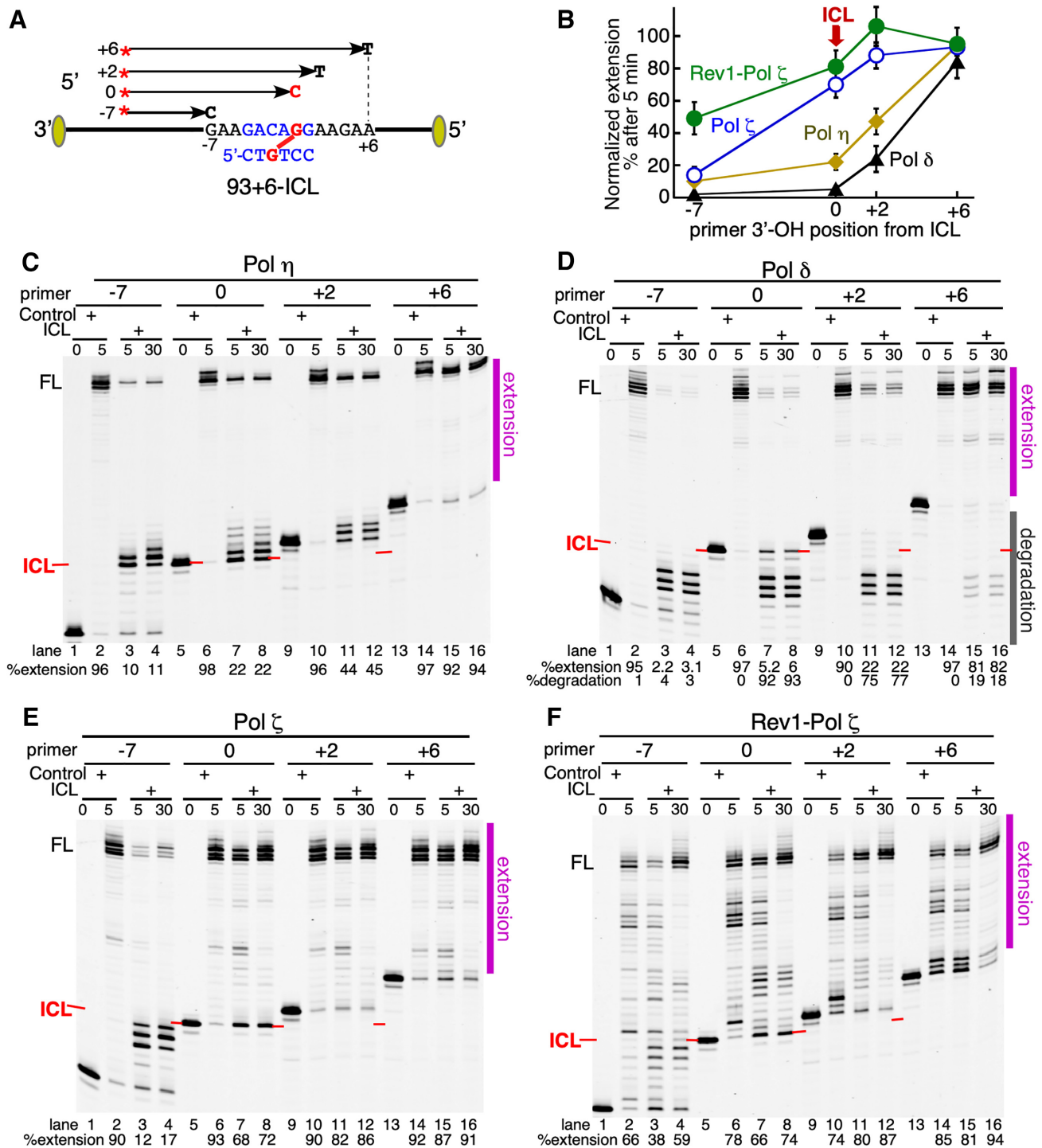


**Figure 5.** Extension of primers hybridized beyond the ICL. (A) The standard primer (-7) and primers at the ICL position (0) and beyond (+2, +6), were used as substrates. (B) The 5 min time points from panels C-F were taken and the normalized % extension (100\*(extension of ICL substrate)/(extension of control substrate)) plotted for each of the primer termini. (C) Pol η. (D) Pol δ. (E) Pol ζ. (F) Rev1-Pol ζ. The products from seven nucleotides beyond the ICL (or the corresponding position on the control template) up to full-length, were defined as extension products and given under each panel. In panel (D), % degradation is defined as the total of all sizes smaller than full primer length. The gray bar to the right of the gel applies to the experiment with the +6 primer only, showing all degradation products generated by Pol δ. FL, full length; see legend to Figure 1 for explanation of migration artifacts.

this experiment, we defined replication product from seven nucleotides past the ICL to full-length as extension products. Thus, elongation of the +6 primer by one nucleotide and more are considered extension products. Quantification of the % of extension by each polymerase is given in Figure 5B. When the series of substrates was tested with Pol  $\eta$ , we saw some improvement in full-length product formation with the +2 primer compared to the standard -7 primer, but stalling was still a major problem (Figure 5C). Only the +6 primer escaped the problem of stalling.

Wild-type Pol  $\delta$  was also tested, in order to determine how far past the ICL its exonuclease activity caused resection of the bypass products (Figure 5D). Pol  $\delta$  extended only the +6 primer efficiently (Figure 5D), suggesting that the double-stranded DNA binding cleft of Pol  $\delta$  is very sensitive to the ICL-induced structural alterations from Watson-Crick base-pairs. Nevertheless, even the +6 substrate was compromised for extension by Pol  $\delta$ . About 20% was subject to degradation by Pol  $\delta$ 's proofreading activity, as follows from the generation of products at positions around the nick (Figure 5B,D). This degradation was observed only with the ICL substrate and not with the control substrate (compare lanes 14 and 15). When the primer was placed only 2 nt beyond the ICL, 75% was degraded back to around the nick position by the proofreading activity of Pol  $\delta$  (lanes 11, 12).

In sharp contrast to what was observed with Pol  $\eta$ , Pol  $\zeta$  extended even the (0) substrate with very high efficiency, while the -7 substrate shows the usual stalling just prior to the ICL (Figure 5E). Rev1-Pol  $\zeta$  similarly extended fully the primer opposite the ICL (0), as well as the +2 and +6 primers (Figure 5F). The continued stalling further downstream of the ICL is a result of the negative regulatory activity of Rev1 on Pol  $\zeta$ , and was also observed with the control template (Figure 5F, e.g. compare lane 10 with 11).

One likely cause for the autoinhibitory activity of Pol  $\eta$  during ICL bypass could be that the 6-mer, which is crosslinked to the template is extended by Pol  $\eta$ . Consequently, after ICL bypass, further elongation would require strand displacement synthesis through the extended 6-mer strand, which would be inhibitory for these TLS polymerases (34). The assay described in Figure 6 lends support to this hypothesis. We incubated a series of DNA substrates, shown in Figure 6A, with Pol  $\eta$ . The 5'-FAM-primer (fluorescein) and its extension products were detected by FAM fluorescence (Figure 6C), while all DNAs were detected with SYBR-gold staining (Figure 6B). The appearance of a Pol  $\eta$ -dependent slow-migrating species with the unprimed 93+6-ICL substrate is evidence that indeed, Pol  $\eta$  used the covalent 6-mer as a primer for extension, yielding an estimated 93+37-ICL product upon replication to the end of the available template (Figure 6B, lane B4). This species was also produced when the primed DNA was replicated by Pol  $\eta$  (lane B6), in addition to elongation of the FAM-primer up to and 1–2 nt past the ICL (lane C6).

Although the 3' hydroxyl group on the unhooked ICL is the substrate generated by nuclease activity, we tested whether blocking extension of the 3' hydroxyl group would lead to a different outcome. We included experiments with a substrate, in which the 3'-terminus of the covalent 6-mer is blocked with a 3'-phosphate, which we generated with

a slight modification of our substrate preparation protocol (Supplementary Figure S6). The result with this template with the blocked 3' hydroxyl group showed, first, that the unprimed ICL DNA is inactive with Pol  $\eta$  (Figure 6B, lane B7), and secondly, that this primed ICL DNA substrate is much more efficiently replicated than the substrate with an unblocked covalent 6-mer (compare lane C8 with C6). Interestingly, while Pol  $\eta$  quantitatively extended the unblocked covalent 6-mer within the time of the assay (5 min, lanes B4, B6), Pol  $\zeta$  elongated only 50–70% of the 6-mer (lanes B9, B11), and Rev1-Pol  $\zeta$  showed little to no activity on the 6-mer (lanes B10, B12). From these studies, we concluded that blocking of the 3'-terminus of the covalent 6-mer would stimulate Pol  $\eta$ -mediated TLS much more than Rev1-Pol  $\zeta$ -mediated bypass. Therefore, we carried out a side-by-side comparison of replication of the ICL substrate with the 6-mer either unblocked or blocked, and with multiple DNA polymerases in the assay, similar to the experiment in Figure 4 (Figure 6D). While Pol  $\eta$ -dependent ICL extension products increased from 15% to 94% upon blocking the 6-mer 3'-terminus (compare lane D2 with D8), and Pol  $\zeta$  extension products increased from 13% to 58% (compare lanes D3 with D9), Rev1-Pol  $\zeta$  extension product showed a more modest improvement, from 50% to 70% (compare lanes D5 with D11). Moreover, whereas the addition of Pol  $\eta$  to an assay with Rev1-Pol  $\zeta$  on the unblocked substrate actually caused a significant inhibition (compare lane D5 with D6), on the blocked substrate, Pol  $\eta$  stimulated Rev1-Pol  $\zeta$  bypass (compare lane D11 with D12).

## DISCUSSION

For over a decade, a consensus model has emerged for TLS in eukaryotic cells (56–58). This process is usually carried out by the tandem action of two DNA polymerases. The first DNA polymerase, the inserter, incorporates one or more nucleotides opposite the lesion, whereas the second DNA polymerase, the extender, continues replication. Depending on the type lesion, the inserter DNA polymerase is usually a Y-family DNA polymerase, such as Pol  $\eta$ , Pol  $\kappa$  or Pol  $\iota$  in mammalian cells, whereas Pol  $\zeta$  is generally considered to be an extender DNA polymerase (1). In yeast, Pol  $\eta$  is the only classical 'inserter' Y-family enzyme. The second Y-family enzyme, Rev1 has a specialized obligatory function with Pol  $\zeta$ , and it does so without generally requiring its unique deoxycytidyl transferase activity, including during TLS of cis-platin induced DNA adducts (59,60). One caveat to these genetic observations with Rev1 is that they do not distinguish between *intra*- and *interstrand* DNA lesions caused by cis-platin.

In our study of a highly replication-blocking ICL, the role of Pol  $\zeta$  as an extender is readily apparent. Once the insertion of a nucleotide across the ICL has been made, extension by Pol  $\zeta$  was facile, regardless of the presence of Rev1 (Figure 5E, F). But the question as to which DNA polymerase is involved in the insertion process remains. Based on Rev1 and Pol  $\zeta$  depletion studies in *Xenopus* egg extracts, Rev1-Pol  $\zeta$  may be responsible for insertion across the ICL, depending on the type of ICL (16,27,33). It is certainly required for the extension step. Therefore, it follows that an

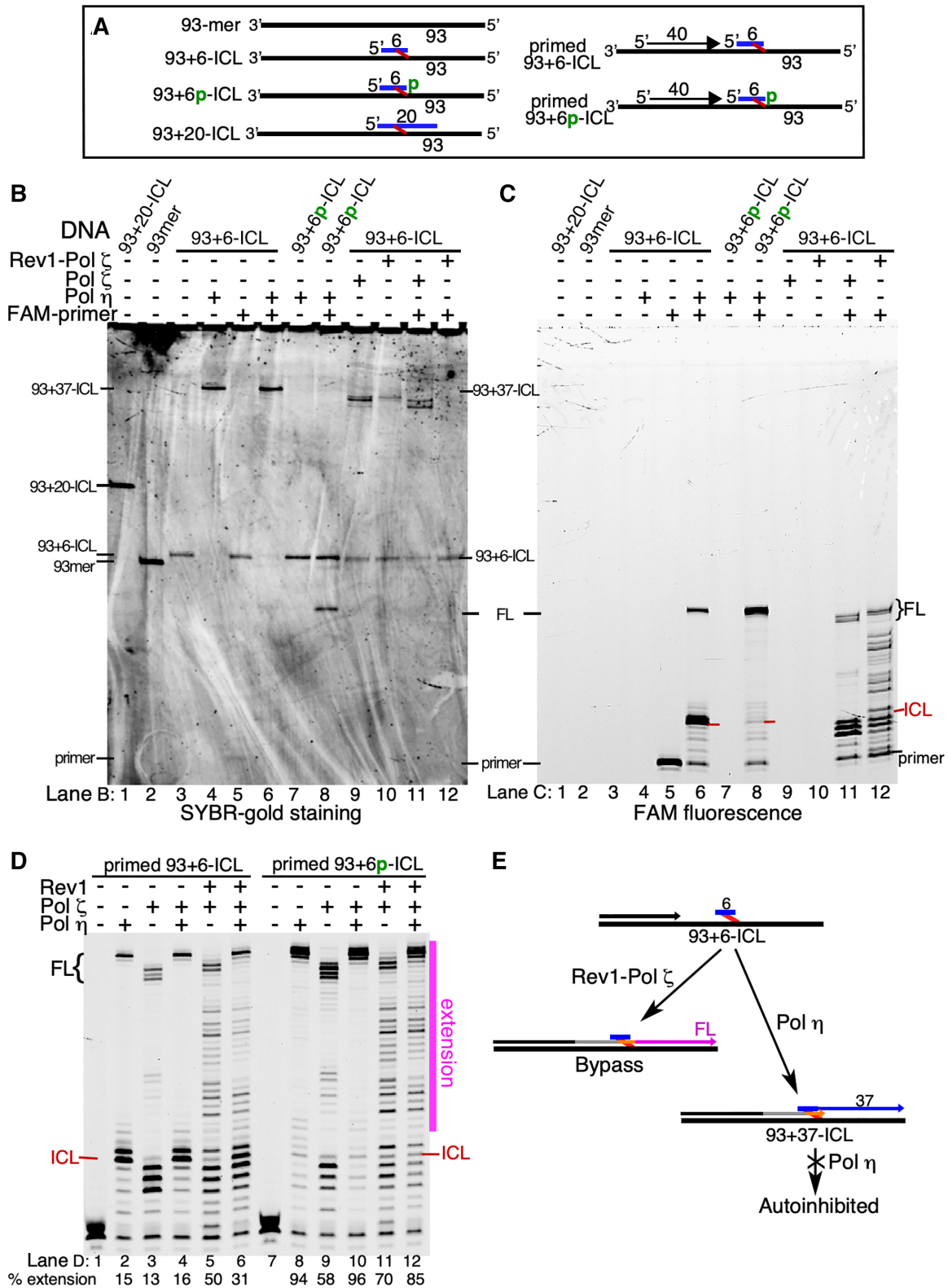


**Figure 6.** Extension of the crosslinked six-mer by Pol η. (A) DNAs used in B and C. All 93mer templates have both 3'- and 5'-biotin-streptavidin blocks. (B, C) Assays were for 5 min at 30°C, and the products analyzed on a 12% PAGE-urea gel, containing 25% formamide. The gel was first scanned in the Typhoon for FAM fluorescence (C), and subsequently stained with SYBR GOLD and scanned in the Typhoon, using the EtBr setting (B). In (B), note that the Pol ζ extension products (lanes B9-B11), do not reach full size because of the presence of the biotin-streptavidin block. Pol η products do reach full size (lanes B4, B6). See also legend to Figure 1B. (D) Standard 5 min assays with the indicated substrates as shown in (A), and combinations of DNA polymerases. (E) Summary of ICL bypass by Pol η and Rev1-Pol ζ. The predominant pathways by each DNA polymerase are indicated.

other DNA polymerase may also be responsible for the insertion step and Rev1–Pol  $\zeta$  for extension.

The purpose of the current study was two-fold. First, to provide a biochemical framework for the activity of Rev1–Pol  $\zeta$  at ICL lesions. While previous studies, including those from our own laboratories, have investigated the biochemical activities of Pol  $\zeta$  and Rev1 at various lesions (12,34), these studies lacked the proper biochemical context, i. e. that of the 5-subunit Rev1–Pol  $\zeta$  complex, together with its essential PCNA clamp, which may additionally be modified by ubiquitination at Lys-164. Secondly, we wanted to investigate which other DNA polymerase could participate in this process as a possible inserter enzyme, using both yeast Pol  $\delta$  and Pol  $\eta$  as candidates. One firm conclusion from our studies is that, under all conditions tested, Pol  $\delta$  was inhibitory to TLS, because of its tendency to degrade TLS insertion and extension intermediates with its proofreading exonuclease activity (Figures 4 and 5D). In fact, as far as six nucleotides past the ICL, the lesion still affects the decision-making process by Pol  $\delta$ , that of extension *versus* degradation (Figure 5D, lanes 14–16). We explored the possibility that ubiquitination of PCNA would reveal a unique step in TLS when multiple DNA polymerases were present. One of the proposed roles of ubiquitination is that it localizes Rev1, and by association Pol  $\zeta$  to the lesion, perhaps favoring the competition between this TLS enzyme and the multitude of other PCNA client proteins for occupancy at the lesion. However, ubiquitinated PCNA did neither stimulate nor inhibit TLS by Rev1–Pol  $\zeta$  in our studies, nor did it disfavor the inhibitory participation by Pol  $\delta$  (Supplementary Figure S5). Studies of the role of PCNA ubiquitination in ICL-TLS in *xenopus* extracts were similarly uninformative (16).

From an enzymatic perspective, Pol  $\eta$  would be an ideal enzyme to serve as an inserter for ICL. In previous studies, Pol  $\eta$  has been shown to replicate past several model ICL lesions (37,61,62), and this is confirmed in the current study. Interestingly, in both the previous and our current studies, Pol  $\eta$  has the propensity to stall either after insertion at ICL, or just past the lesion (Figure 1D). This would provide an ideal intermediate for a hand-off of intermediate from Pol  $\eta$  to Pol  $\zeta$  or Rev1–Pol  $\zeta$ . Our control studies show that, at least for this ICL substrate, the source of the inhibition could be attributed to an off-target reaction, i.e. the extension of the ICL-associated covalent hexanucleotide by Pol  $\eta$ . While this Pol  $\eta$ -mediated extension of the ICL 6-mer also causes inhibits further bypass and extension by Pol  $\eta$  itself (Figures 1E and 4B), more importantly, it forms an almost complete block for extension by Pol  $\zeta$  or Rev1–Pol  $\zeta$  (Figure 4B). Therefore, a two-enzyme TLS model involving Pol  $\eta$  and Rev1–Pol  $\zeta$  would only be efficient if either the off-target extension were prevented, most likely by a protein blocking the extension of the unhooked ICL, or it could be remedied by a nuclease such as Pso2/SNM1A (63,64), which would iteratively cut the attached ICL strand being elongated by Pol  $\eta$ . Alternatively, the required strand displacement synthesis by Rev1–Pol  $\zeta$  through the downstream double-stranded DNA could be facilitated for example by a DNA helicase. As a further complication, the genetic evidence for the involvement of Pol  $\eta$  (*RAD30*) in ICL repair in yeast is not strong. A yeast *rad30* $\Delta$  mutant showed no sensitivity to a variety of ICLs (18,65,66). Furthermore,

loss of *RAD30* showed no effect on the hypermutability to cis-platin (67). By contrast, POLH deficient DT40 cells or XPV patients cells are mildly sensitive to cisplatin, consistent with a possible role of vertebrate Pol  $\eta$  in ICL repair, perhaps redundant with another polymerase (21,68).

Our studies indicate that Rev1–Pol  $\zeta$  may function as both an inserter and extender. Rev1 stimulated the synthesis of substantial percentage of extension products by Pol  $\zeta$ , in a process which is only in part dependent on the catalytic activity of Rev 1 (Figure 2). Our data on the dispensability of Rev1's catalytic activity are consistent with a genetic study, which shows that the catalytic inactive mutant of Rev1 does not sensitize yeast to treatment with *cis*-platin (60). Of importance for successful TLS is that the primer terminus is in close proximity to the ICL upon the recruitment of Rev1–Pol  $\zeta$  (Figure 3). The function of Rev1 on non-damaged DNA is to inhibit DNA synthesis by Pol  $\zeta$ , and this can be observed in all of our experiments. Therefore, engaging Rev1–Pol  $\zeta$  too far from the ICL may result in premature stalling of the complex. Conversely, Rev1 also ensures that TLS is terminated soon after lesion bypass has been accomplished. While this type of regulation by Rev1 makes sense from a physiological point of view, our biochemical data cannot be easily be reconciled with a recent study, which suggests that Pol  $\zeta$  can carry out extensive TLS in yeast, for stretches longer than 200 nucleotides, and introduce mutations during this process (69). Currently, it is not clear whether these extended mutagenic stretches are the result of processive DNA synthesis by Pol  $\zeta$ , perhaps after dissociation of Rev1, or the result of iterative binding of Rev1–Pol  $\zeta$  on the gapped, damaged DNA, resulting in close, but individual mutational patches.

Cells with mutations in Pol  $\zeta$  are among the most hypersensitive to ICL-forming agents, and here we show that Rev1–Pol  $\zeta$  can function as both an inserter and extender polymerase in bypassing ICLs. Our results further suggest that that in a physiological context, the insertion step across ICL may be aided by another DNA polymerase such as Pol  $\eta$ . The limited sensitivity of Pol  $\eta$  deficient cells suggests that this function may be redundant with an additional TLS polymerase. The definitive answer to this question will have to await better biochemical systems to study ICL repair in yeast or human cells or conversely, improved genetics in *Xenopus laevis*, allowing for the generation of multiple simultaneous mutations in ICL repair genes in egg extracts that provide the only trackable biochemical system to study ICL repair to date. In the meantime, our studies provide a framework for the understanding of the role of Rev1–Pol  $\zeta$  in ICL repair.

## SUPPLEMENTARY DATA

Supplementary Data are available at NAR Online.

## ACKNOWLEDGEMENTS

We thank Arnold S. Groehler IV (IBS Center for Genomic Integrity) for analyzing ICL-containing oligonucleotides by LC–MS.

*Author contributions:* R.B.B., Y.K.C., U.R., O.D.S. and P.M.B. planned this study. Y.K.C. and U.R. synthesized

the substrates and R.B.B. carried out the enzymatic studies. R.B.B., Y.K.C., O.D.S. and P.M.B. were involved in the interpretation of the results and the writing of the paper. All authors approved of the final version.

## FUNDING

National Institutes of Health [GM118129 to P.M.B., CA165911 to O.D.S., in part]; Korean Institute for Basic Science [IBS-R022-A1 to O.D.S.]. Funding for open access charge: NIGMS [118129].

*Conflict of interest statement.* None declared.

## REFERENCES

- Martin, S.K. and Wood, R.D. (2019) DNA polymerase zeta in DNA replication and repair. *Nucleic Acids Res.*, **47**, 8348–8361.
- Johnson, R.E., Washington, M.T., Haracska, L., Prakash, S. and Prakash, L. (2000) Eukaryotic polymerases  $\iota$  and  $\zeta$  act sequentially to bypass DNA lesions. *Nature*, **406**, 1015–1019.
- Zhong, X., Garg, P., Stith, C.M., McElhinny, S.A., Kissling, G.E., Burgers, P.M. and Kunkel, T.A. (2006) The fidelity of DNA synthesis by yeast DNA polymerase  $\zeta$  alone and with accessory proteins. *Nucleic Acids Res.*, **34**, 4731–4742.
- Johnson, R.E., Prakash, L. and Prakash, S. (2012) Pol31 and Pol32 subunits of yeast DNA polymerase  $\delta$  are also essential subunits of DNA polymerase  $\zeta$ . *Proc. Natl Acad. Sci. U.S.A.*, **109**, 12455–12460.
- Makarova, A.V., Stodola, J.L. and Burgers, P.M. (2012) A four-subunit DNA polymerase  $\zeta$  complex containing Pol  $\delta$  accessory subunits is essential for PCNA-mediated mutagenesis. *Nucleic Acids Res.*, **40**, 11618–11626.
- Kochanova, O.V., Bezalel-Buch, R., Tran, P., Makarova, A.V., Chabes, A., Burgers, P.M. and Shcherbakova, P.V. (2017) Yeast DNA polymerase  $\zeta$  maintains consistent activity and mutagenicity across a wide range of physiological dNTP concentrations. *Nucleic Acids Res.*, **45**, 1200–1218.
- Rizzo, A.A., Vassel, F.M., Chatterjee, N., D'Souza, S., Li, Y., Hao, B., Hemann, M.T., Walker, G.C. and Korzhnev, D.M. (2018) Rev7 dimerization is important for assembly and function of the Rev1/Polzeta translesion synthesis complex. *Proc. Natl Acad. Sci. U.S.A.*, **115**, E8191–E8200.
- Tomida, J., Takata, K., Lange, S.S., Schibler, A.C., Yousefzadeh, M.J., Bhetawal, S., Dent, S.Y. and Wood, R.D. (2015) REV7 is essential for DNA damage tolerance via two REV3L binding sites in mammalian DNA polymerase  $\zeta$ . *Nucleic Acids Res.*, **43**, 1000–1011.
- Garg, P., Stith, C.M., Majka, J. and Burgers, P.M. (2005) Proliferating cell nuclear antigen promotes translesion synthesis by DNA polymerase  $\zeta$ . *J. Biol. Chem.*, **280**, 23446–23450.
- Nelson, J.R., Lawrence, C.W. and Hinkle, D.C. (1996) Deoxycytidyl transferase activity of yeast rev1 protein. *Nature*, **382**, 729–731.
- Lemontt, J.F. (1971) Mutants of yeast defective in mutation induced by ultraviolet light. *Genetics*, **68**, 21–33.
- Haracska, L., Unk, I., Johnson, R.E., Johansson, E., Burgers, P.M., Prakash, S. and Prakash, L. (2001) Roles of yeast DNA polymerases  $\delta$  and  $\zeta$  and of Rev1 in the bypass of abasic sites. *Genes Dev.*, **15**, 945–954.
- Garg, P. and Burgers, P.M. (2005) Ubiquitinated proliferating cell nuclear antigen activates translesion DNA polymerases  $\epsilon$  and REV1. *Proc. Natl Acad. Sci. U.S.A.*, **102**, 18361–18366.
- Northam, M.R., Garg, P., Baitin, D.M., Burgers, P.M. and Shcherbakova, P.V. (2006) A novel function of DNA polymerase  $\zeta$  regulated by PCNA. *EMBO J.*, **25**, 4316–4325.
- Wood, A., Garg, P. and Burgers, P.M. (2007) A ubiquitin-binding motif in the translesion DNA polymerase Rev1 mediates its essential functional interaction with ubiquitinated proliferating cell nuclear antigen in response to DNA damage. *J. Biol. Chem.*, **282**, 20256–20263.
- Budzowska, M., Graham, T.G., Sobek, A., Waga, S. and Walter, J.C. (2015) Regulation of the Rev1-pol  $\zeta$  complex during bypass of a DNA interstrand cross-link. *EMBO J.*, **34**, 1971–1985.
- Powers, K.T. and Washington, M.T. (2018) Eukaryotic translesion synthesis: choosing the right tool for the job. *DNA Repair (Amst.)*, **71**, 127–134.
- Sarkar, S., Davies, A.A., Ulrich, H.D. and McHugh, P.J. (2006) DNA interstrand crosslink repair during G1 involves nucleotide excision repair and DNA polymerase  $\zeta$ . *EMBO J.*, **25**, 1285–1294.
- Ho, T.V. and Scharer, O.D. (2010) Translesion DNA synthesis polymerases in DNA interstrand crosslink repair. *Environ. Mol. Mutagen.*, **51**, 552–566.
- Kim, H., Yang, K., Dejsuphong, D. and D'Andrea, A.D. (2012) Regulation of Rev1 by the Fanconi anemia core complex. *Nat. Struct. Mol. Biol.*, **19**, 164–170.
- Nojima, K., Hohegger, H., Saberi, A., Fukushima, T., Kikuchi, K., Yoshimura, M., Orelli, B.J., Bishop, D.K., Hirano, S., Ohzeki, M. et al. (2005) Multiple repair pathways mediate tolerance to chemotherapeutic cross-linking agents in vertebrate cells. *Cancer Res.*, **65**, 11704–11711.
- Shen, X., Jun, S., O'Neal, L.E., Sonoda, E., Bemark, M., Sale, J.E. and Li, L. (2006) REV3 and REV1 play major roles in recombination-independent repair of DNA interstrand cross-links mediated by monoubiquitinated proliferating cell nuclear antigen (PCNA). *J. Biol. Chem.*, **281**, 13869–13872.
- Sonoda, E., Okada, T., Zhao, G.Y., Tateishi, S., Araki, K., Yamaizumi, M., Yagi, T., Verkaik, N.S., van Gent, D.C., Takata, M. et al. (2003) Multiple roles of Rev3, the catalytic subunit of polzeta in maintaining genome stability in vertebrates. *EMBO J.*, **22**, 3188–3197.
- Clauson, C., Scharer, O.D. and Niedernhofer, L. (2013) Advances in understanding the complex mechanisms of DNA interstrand cross-link repair. *Cold Spring Harb. Perspect. Biol.*, **5**, a012732.
- Roy, U. and Scharer, O.D. (2016) Involvement of translesion synthesis DNA polymerases in DNA interstrand crosslink repair. *DNA Repair (Amst.)*, **44**, 33–41.
- Deans, A.J. and West, S.C. (2011) DNA interstrand crosslink repair and cancer. *Nat. Rev. Cancer*, **11**, 467–480.
- Raschle, M., Knipscheer, P., Enoiu, M., Angelov, T., Sun, J., Griffith, J.D., Ellenberger, T.E., Scharer, O.D. and Walter, J.C. (2008) Mechanism of replication-coupled DNA interstrand crosslink repair. *Cell*, **134**, 969–980.
- Huang, J., Liu, S., Bellani, M.A., Thazhathveetil, A.K., Ling, C., de Winter, J.P., Wang, Y., Wang, W. and Seidman, M.M. (2013) The DNA translocase FANCM/MHF promotes replication traverse of DNA interstrand crosslinks. *Mol. Cell*, **52**, 434–446.
- Klein Douwel, D., Boonen, R.A., Long, D.T., Szypowska, A.A., Raschle, M., Walter, J.C. and Knipscheer, P. (2014) XPF-ERCC1 acts in unhooking DNA interstrand crosslinks in cooperation with FANCD2 and FANCP/SLX4. *Mol. Cell*, **54**, 460–471.
- Knipscheer, P., Raschle, M., Smogorzewska, A., Enoiu, M., Ho, T.V., Scharer, O.D., Elledge, S.J. and Walter, J.C. (2009) The Fanconi anemia pathway promotes replication-dependent DNA interstrand cross-link repair. *Science*, **326**, 1698–1701.
- Wang, A.T., Sengerova, B., Cattell, E., Inagawa, T., Hartley, J.M., Kiakos, K., Burgess-Brown, N.A., Swift, L.P., Enzlin, J.H., Schofield, C.J. et al. (2011) Human SNM1A and XPF-ERCC1 collaborate to initiate DNA interstrand cross-link repair. *Genes Dev.*, **25**, 1859–1870.
- Semlow, D.R., Zhang, J., Budzowska, M., Drohat, A.C. and Walter, J.C. (2016) Replication-dependent unhooking of DNA interstrand cross-links by the NEIL3 glycosylase. *Cell*, **167**, 498–511.
- Hodskinson, M.R., Bolner, A., Sato, K., Kamimae-Lanning, A.N., Rooijers, K., Witte, M., Mahesh, M., Silhan, J., Petek, M., Williams, D.M. et al. (2020) Alcohol-derived DNA crosslinks are repaired by two distinct mechanisms. *Nature*, **579**, 603–608.
- Ho, T.V., Guainazzi, A., Derkunt, S.B., Enoiu, M. and Scharer, O.D. (2011) Structure-dependent bypass of DNA interstrand crosslinks by translesion synthesis polymerases. *Nucleic Acids Res.*, **39**, 7455–7464.
- Minko, I.G., Harbut, M.B., Kozekov, I.D., Kozekova, A., Jakobs, P.M., Olson, S.B., Moses, R.E., Harris, T.M., Rizzo, C.J. and Lloyd, R.S. (2008) Role for DNA polymerase  $\kappa$  in the processing of N2-N2-guanine interstrand cross-links. *J. Biol. Chem.*, **283**, 17075–17082.
- Beagan, K., Armstrong, R.L., Witsell, A., Roy, U., Renedo, N., Baker, A.E., Scharer, O.D. and McVey, M. (2017) Drosophila DNA polymerase  $\theta$  utilizes both helicase-like and polymerase domains

- during microhomology-mediated end joining and interstrand crosslink repair. *PLoS Genet.*, **13**, e1006813.
37. Roy, U., Mukherjee, S., Sharma, A., Frank, E.G. and Scharer, O.D. (2016) The structure and duplex context of DNA interstrand crosslinks affects the activity of DNA polymerase  $\epsilon$ . *Nucleic Acids Res.*, **44**, 7281–7291.
  38. Angelov, T., Guainazzi, A. and Scharer, O.D. (2009) Generation of DNA interstrand cross-links by post-synthetic reductive amination. *Org. Lett.*, **11**, 661–664.
  39. Fortune, J.M., Stith, C.M., Kissling, G.E., Burgers, P.M. and Kunkel, T.A. (2006) RPA and PCNA suppress formation of large deletion errors by yeast DNA polymerase  $\delta$ . *Nucleic Acids Res.*, **34**, 4335–4341.
  40. Henricksen, L.A., Umbricht, C.B. and Wold, M.S. (1994) Recombinant replication protein A: expression, complex formation, and functional characterization. *J. Biol. Chem.*, **269**, 11121–11132.
  41. Gerik, K.J., Gary, S.L. and Burgers, P.M. (1997) Overproduction and affinity purification of *Saccharomyces cerevisiae* replication factor C. *J. Biol. Chem.*, **272**, 1256–1262.
  42. Ayyagari, R., Impellizzeri, K.J., Yoder, B.L., Gary, S.L. and Burgers, P.M. (1995) A mutational analysis of the Yeast proliferating cell nuclear antigen indicates distinct roles in DNA replication and DNA repair. *Mol. Cell Biol.*, **15**, 4420–4429.
  43. Stodola, J.L. and Burgers, P.M. (2016) Resolving individual steps of Okazaki-fragment maturation at a millisecond timescale. *Nat. Struct. Mol. Biol.*, **23**, 402–408.
  44. Mukherjee, S., Guainazzi, A. and Scharer, O.D. (2014) Synthesis of structurally diverse major groove DNA interstrand crosslinks using three different aldehyde precursors. *Nucleic Acids Res.*, **42**, 7429–7435.
  45. Garg, P., Stith, C.M., Sabouri, N., Johansson, E. and Burgers, P.M. (2004) Idling by DNA polymerase  $\delta$  maintains a ligatable nick during lagging-strand DNA replication. *Genes Dev.*, **18**, 2764–2773.
  46. Mogi, S., Butcher, C.E. and Oh, D.H. (2008) DNA polymerase  $\epsilon$  reduces the gamma-H2AX response to psoralen interstrand crosslinks in human cells. *Exp. Cell Res.*, **314**, 887–895.
  47. McCulloch, S.D., Kokoska, R.J., Chilkova, O., Welch, C.M., Johansson, E., Burgers, P.M. and Kunkel, T.A. (2004) Enzymatic switching for efficient and accurate translesion DNA replication. *Nucleic Acids Res.*, **32**, 4665–4675.
  48. Kusumoto, R., Masutani, C., Shimmyo, S., Iwai, S. and Hanaoka, F. (2004) DNA binding properties of human DNA polymerase  $\epsilon$ : implications for fidelity and polymerase switching of translesion synthesis. *Genes Cells*, **9**, 1139–1150.
  49. Shachar, S., Ziv, O., Avkin, S., Adar, S., Wittschieben, J., Reissner, T., Chaney, S., Friedberg, E.C., Wang, Z., Carell, T. *et al.* (2009) Two-polymerase mechanisms dictate error-free and error-prone translesion DNA synthesis in mammals. *EMBO J.*, **28**, 383–393.
  50. Washington, M.T., Minko, I.G., Johnson, R.E., Wolffe, W.T., Harris, T.M., Lloyd, R.S., Prakash, S. and Prakash, L. (2004) Efficient and error-free replication past a minor-groove DNA adduct by the sequential action of human DNA polymerases  $\iota$  and  $\kappa$ . *Mol. Cell Biol.*, **24**, 5687–5693.
  51. Saribasak, H., Maul, R.W., Cao, Z., Yang, W.W., Schenten, D., Kracker, S. and Gearhart, P.J. (2012) DNA polymerase  $\zeta$  generates tandem mutations in immunoglobulin variable regions. *J. Exp. Med.*, **209**, 1075–1081.
  52. Hoegge, C., Pfander, B., Moldovan, G.L., Pyrowolakis, G. and Jentsch, S. (2002) RAD6-dependent DNA repair is linked to modification of PCNA by ubiquitin and SUMO. *Nature*, **419**, 135–141.
  53. Bienko, M., Green, C.M., Crosetto, N., Rudolf, F., Zapart, G., Coull, B., Kannouche, P., Wider, G., Peter, M., Lehmann, A.R. *et al.* (2005) Ubiquitin-binding domains in Y-family polymerases regulate translesion synthesis. *Science*, **310**, 1821–1824.
  54. Bomar, M.G., D'Souza, S., Bienko, M., Dikic, I., Walker, G.C. and Zhou, P. (2010) Unconventional ubiquitin recognition by the ubiquitin-binding motif within the Y family DNA polymerases  $\iota$  and Rev1. *Mol. Cell*, **37**, 408–417.
  55. Guillian, T.A. and Yeeles, J.T.P. (2020) Reconstitution of translesion synthesis reveals a mechanism of eukaryotic DNA replication restart. *Nat. Struct. Mol. Biol.*, **27**, 450–460.
  56. Livneh, Z., Ziv, O. and Shachar, S. (2010) Multiple two-polymerase mechanisms in mammalian translesion DNA synthesis. *Cell Cycle*, **9**, 729–735.
  57. Vaisman, A. and Woodgate, R. (2017) Translesion DNA polymerases in eukaryotes: what makes them tick? *Crit. Rev. Biochem. Mol. Biol.*, **52**, 274–303.
  58. Zhao, L. and Washington, M.T. (2017) Translesion Synthesis: Insights into the selection and switching of DNA polymerases. *Genes (Basel)*, **8**, 24.
  59. Ross, A.L., Simpson, L.J. and Sale, J.E. (2005) Vertebrate DNA damage tolerance requires the C-terminus but not BRCT or transferase domains of REV1. *Nucleic Acids Res.*, **33**, 1280–1289.
  60. Wiltout, M.E. and Walker, G.C. (2011) The DNA polymerase activity of *Saccharomyces cerevisiae* Rev1 is biologically significant. *Genetics*, **187**, 21–35.
  61. Klug, A.R., Harbut, M.B., Lloyd, R.S. and Minko, I.G. (2012) Replication bypass of N2-deoxyguanosine interstrand cross-links by human DNA polymerases  $\epsilon$  and  $\iota$ . *Chem. Res. Toxicol.*, **25**, 755–762.
  62. Xu, W., Ouellette, A., Ghosh, S., O'Neill, T.C., Greenberg, M.M. and Zhao, L. (2015) Mutagenic bypass of an oxidized abasic Lesion-Induced DNA interstrand Cross-Link analogue by human translesion synthesis DNA polymerases. *Biochemistry*, **54**, 7409–7422.
  63. Sengerova, B., Wang, A.T. and McHugh, P.J. (2011) Orchestrating the nucleases involved in DNA interstrand cross-link (ICL) repair. *Cell Cycle*, **10**, 3999–4008.
  64. Zhang, J. and Walter, J.C. (2014) Mechanism and regulation of incisions during DNA interstrand cross-link repair. *DNA Repair (Amst.)*, **19**, 135–142.
  65. Grossmann, K.F., Ward, A.M., Matkovic, M.E., Folias, A.E. and Moses, R.E. (2001) *S. cerevisiae* has three pathways for DNA interstrand crosslink repair. *Mutat. Res.*, **487**, 73–83.
  66. De La Rosa, V.Y., Asfaha, J., Fasullo, M., Loguinov, A., Li, P., Moore, L.E., Rothman, N., Nakamura, J., Swenberg, J.A., Scelo, G. *et al.* (2017) Editor's Highlight: High-Throughput functional genomics identifies modulators of TCE metabolite genotoxicity and candidate susceptibility genes. *Toxicol. Sci.*, **160**, 111–120.
  67. Segovia, R., Shen, Y., Lujan, S.A., Jones, S.J. and Stirling, P.C. (2017) Hypermutation signature reveals a slippage and realignment model of translesion synthesis by Rev3 polymerase in cisplatin-treated yeast. *Proc. Natl Acad. Sci. U.S.A.*, **114**, 2663–2668.
  68. Albertella, M.R., Green, C.M., Lehmann, A.R. and O'Connor, M.J. (2005) A role for polymerase  $\epsilon$  in the cellular tolerance to cisplatin-induced damage. *Cancer Res.*, **65**, 9799–9806.
  69. Kochenova, O.V., Dae, D.L., Mertz, T.M. and Shcherbakova, P.V. (2015) DNA polymerase  $\zeta$ -dependent lesion bypass in *Saccharomyces cerevisiae* is accompanied by error-prone copying of long stretches of adjacent DNA. *PLoS Genet.*, **11**, e1005110.

## **Supplemental information to:**

### **Bypass of DNA Interstrand crosslinks by a Rev1-DNA polymerase $\zeta$ complex.**

Rachel Bezalel-Buch<sup>1</sup>, Young K. Cheun<sup>2</sup>, Upasana Roy<sup>3,4</sup>, Orlando D. Schärer<sup>2,5</sup> and Peter M. Burgers<sup>1\*</sup>

<sup>1</sup> Department of Biochemistry and Molecular Biophysics, Washington University School of Medicine, Saint Louis, Missouri, USA, <sup>2</sup> Center for Genomic Integrity, Institute for Basic Science, Ulsan, 44919, Republic of Korea, <sup>3</sup> Department of Chemistry, Stony Brook University, Stony Brook, NY 11794, USA, <sup>4</sup>Department of Biochemistry & Molecular Biophysics, Columbia University, New York, NY, 10032, USA, <sup>5</sup>Department of Biological Sciences, School of Life Sciences, Ulsan National Institute of Science and Technology, Ulsan, 44919, Republic of Korea

\*Corresponding author: TEL (314) 362-3772; FAX (314) 362-7183; [burgers@wustl.edu](mailto:burgers@wustl.edu)

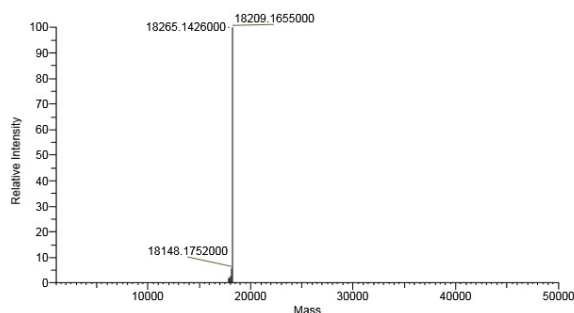
**Table S1. Sequences of DNA substrates and oligonucleotides**

Name	Sequence
<i>DNA substrates:</i>	
Control undamaged 93mer	5'-bio-CACTAGACGAAGCTTGATATGGGCGAAAGAAGGACAG AAGAGGGTACCATCATAGAGTCAGTGGGCATTCAAGTGACGGGTACCATAGTCACG-3'-bio
93+6-ICL	5'-bio-CACTAGACGAAGCTTGATATGGGCGAAAGAAG <b>GACAG</b> AAGAGGGTACCATCATAGAGTCAGTGGGCATTCAAGTGACGGGTACCATAGTCACG-3'-bio ,crosslinked to: 5'- <b>pCTGTCC</b>
93+20-ICL	5'-bio-CACTAGACGAAGCTTGATATGGGCGAAAGAAG <b>GACAG</b> AAGAGGGTACCATCATAGAGTCAGTGGGCATTCAAGTGACGGGTACCATAGTCACG-3'-bio ,crosslinked to 5'-CCCTCTT <b>CTGTCC</b> TTCTTTC
93+6 <b>p</b> -ICL	5'-bio-CACTAGACGAAGCTTGATATGGGCGAAAGAAG <b>GACAG</b> AAGAGGGTACCATCATAGAGTCAGTGGGCATTCAAGTGACGGGTACCATAGTCACG-3'-bio ,crosslinked to: 5'- <b>pCTGTCCp</b> -3'
<i>Fluorescent labeled primers:</i>	
P40-20	5' FAM-CGTGACTATGGTACCCGTCACTTGAATGCCACTGACTCT
P40 -9	5' FAM-ACCCGTCACTTGAATGCCACTGACTCTATGATGGTACCC
P40 -7	5' FAM-CCGTCACTTGAATGCCACTGACTCTATGATGGTACCCCT
P46 (0)	5' FAM-CCGTCACTTGAATGCCACTGACTCTATGATGGTACCCCTTCTGT <b>C</b>
P48 (+2)	5' FAM-CCGTCACTTGAATGCCACTGACTCTATGATGGTACCCCTTCTGT <b>CT</b>
P52 (+6)	5' FAM-CCGTCACTTGAATGCCACTGACTCTATGATGGTACCCCTTCTGT <b>CTTCTT</b>
<i>Biotinylated extension oligonucleotides:</i>	
5'ext	5'-bio-CACTAGACGAAGCTTGATATGGGC
3'ext	5'- <b>p</b> GGCATTC AAGTGACGGGTACCATAGTCACG-3'-bio
<i>Splint oligonucleotides:</i>	
5'splint	5'-TCTTTGCGCCATATCAAGCTTC
3'splint	5'-CACTTGAATGCCACTGACTC
<i>39mer ICLs:</i>	
39+20(6)-ICL	5'-GAAAGAAG <b>G</b> ACAGAAGAGGGTACCATCATAGAGTCAGTG, crosslinked to 5'-CCCTCTUCT <b>G</b> TCCUTCTTTC
39+6-ICL	5'-GAAAGAAG <b>G</b> ACAGAAGAGGGTACCATCATAGAGTCAGTG, crosslinked to 5'- <b>pCTGTCCp</b> -3'
<i>Template oligonucleotides:</i>	
T39-G	5'-GAAAGAAGGACAGAAGAGGGTACCATCATAGAGTCAGTG
T39-C2	5'-GAAAGAAG <b>X</b> ACAGAAGAGGGTACCATCATAGAGTCAGTG
T93-C2	5'-bio-CACTAGACGAAGCTTGATATGGGCGAAAGAAG <b>X</b> ACAG AAGAGGGTACCATCATAGAGTCAGTGGGCATTCAAGTGACGGGTACCATAGTCACG-3'-bio
C20-C2	5'-CCCTCTTCT <b>X</b> TCCTTCTTTC

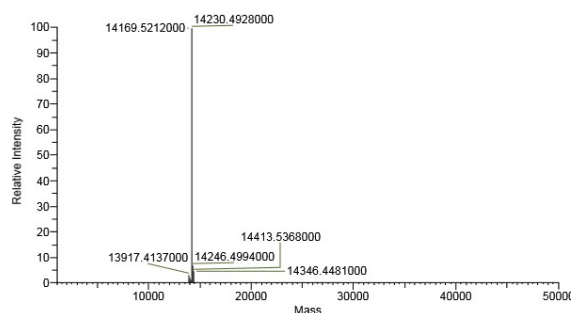
\*Note: Bold, red G indicates the crosslink position of ICL; bold, red C: C opposite the crosslinked residue; bold X: ICL precursor; bio: biotin; p: phosphate; FAM: fluorescein.

**A**

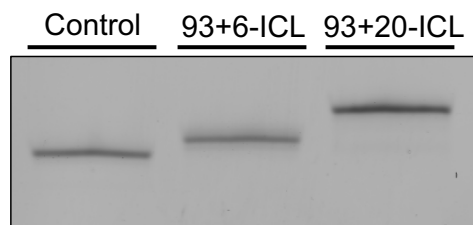
Name	Calculated Mass	Observed Mass	Accuracy
39+20(6)-ICL	18209.175	18209.1655	$\pm 0.522$ ppm
39+6-ICL	14230.497	14230.4928	$\pm 0.295$ ppm



Deconvoluted spectrum of  
39+20(6)-ICL



Deconvoluted spectrum of  
39+6-ICL

**B**

**Figure S1. Analysis of the DNA substrates used in this study. (A)** LC-MS analysis of ICL intermediates. UPLC-ESI-MS analyses were conducted with a Thermo Scientific Q-Exactive Focus hybrid quadrupole-Orbitrap mass spectrometer interfaced with a Thermo Scientific UltiMate 3000 UHPLC system. A heated electrospray ionization (HESI-II) probe was operated in negative ionization mode. The analyzer was operated in full-MS mode with a scan range of  $m/z$  200 – 2000. A Thermo Scientific Hypersil GOLD (100 x 2.1 mm, 1.9  $\mu$ m) column was conditioned with 15mM ammonium acetate and acetonitrile at 40 °C at a flow rate of 50  $\mu$ L/min. DNA oligo (50 pmol) was eluted with a gradient that was initially kept at 2% acetonitrile for 2 minutes, then linearly increased to 80% acetonitrile over 16 minutes, kept at 80% acetonitrile for 2 minutes, decreased to 2% acetonitrile over 2 minutes, and finally re-equilibrated at 2% acetonitrile for 13 minutes. Under these conditions, DNA oligos eluted between 14 – 16 minutes. Spectral data was deconvoluted using Thermo Scientific BioPharma Finder 3.1 software. **(B)** 0.5 pmol of the purified 93mer substrates (Figure 1A, Table S1) were loaded to a 10% polyacrylamide gel containing 7 M urea and 1X TBE. The resolved gel was stained with SYBR gold (Thermo Scientific) and visualized by biomolecular imager (GE Typhoon FLA 7000).

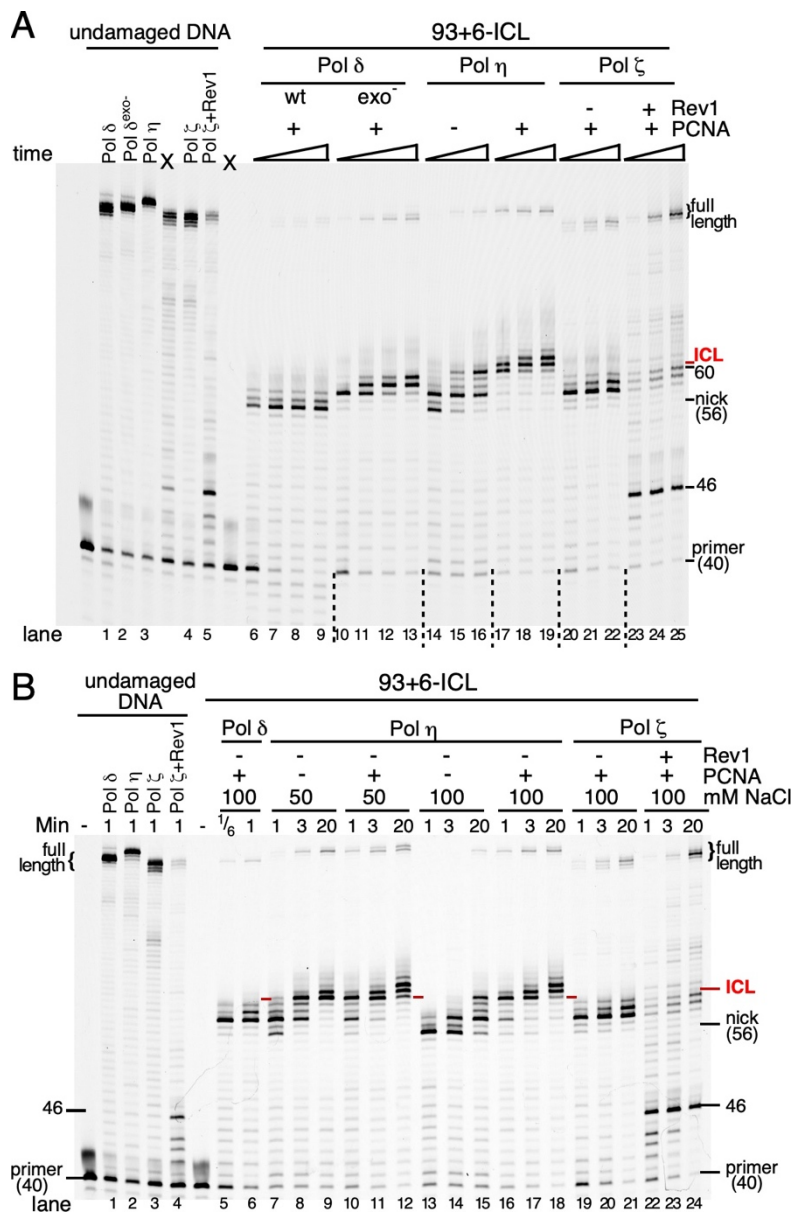


**Figure S2. Translesion DNA synthesis of an ICL by yeast DNA polymerases. (A)** This is the entire gel, which was cut up for easier visualization in Figure 1C. Lanes removed are indicated with an X. **(B)** Time course of replication of control DNA (left section) or ICL DNA. Assays with Pol  $\eta$  were performed at the indicated concentrations of NaCl and either with or without PCNA. Assays with Pol  $\delta$  and Pol  $\zeta$ , the latter with or without Rev1, were performed at 100 mM NaCl.

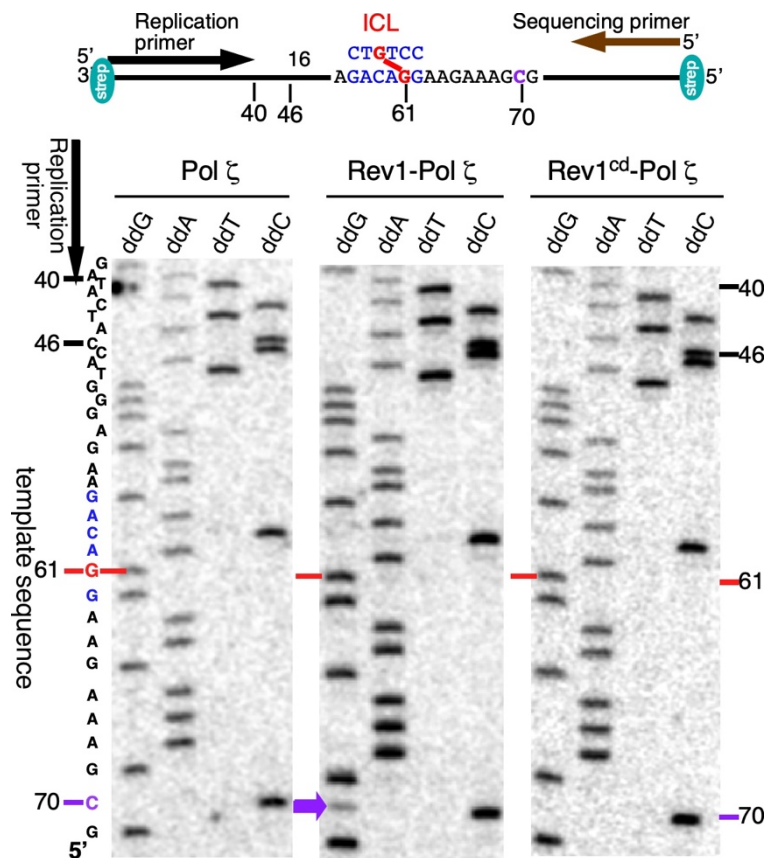


**Figure S3. Sequencing of TLS products.** Extended sequencing reaction of the section shown in Fig. 2C. Top, schematic map of the assay. Full-length replication products were isolated from 60 min assays. Bottom, sequencing analysis. The red arrow indicates the ICL-dG template position, which is replicated by insertion of dCMP, which is sequenced as a dG. The purple arrow at position 70 indicates a position where Rev1, but not Rev1<sup>Δd</sup> misincorporates dCMP across from template dC with a frequency of 15-20%. Note that at the major template dC stall site at position 46, dGMP is faithfully incorporated opposite the dC template.

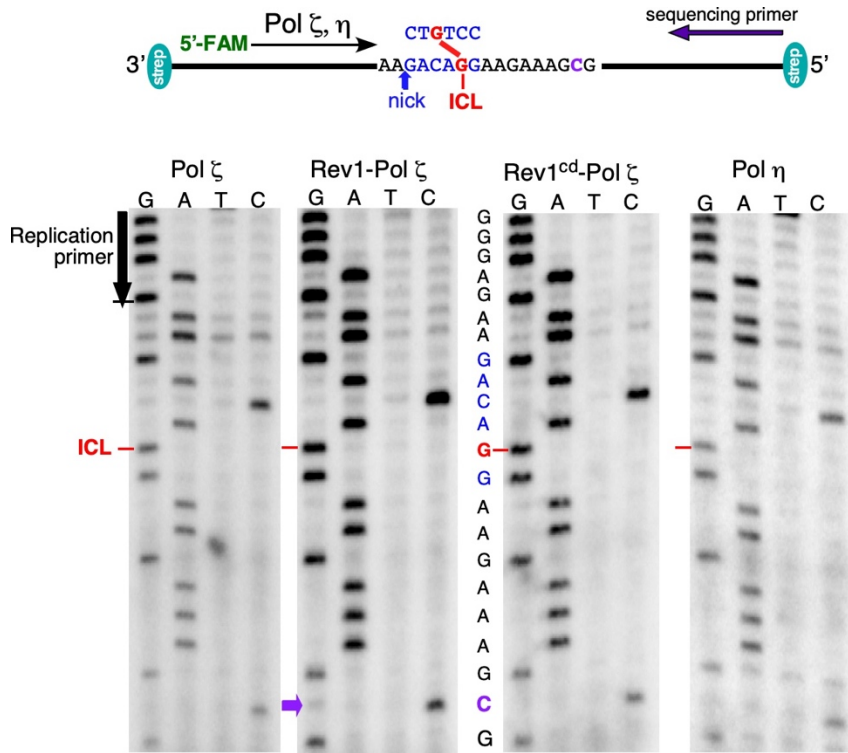


**Figure S4. Sequencing of TLS products.** Top, schematic map of the assay. See Fig. 3 for TLS assay. Bottom, sequencing analysis. Full-length replication products were isolated from 60 min assays. The red arrow indicates the ICL-dG template position, which is replicated by insertion of dCMP, which is sequenced as a dG. The purple arrow at position 70 indicates a position where Rev1, but not Rev1<sup>cd</sup> misincorporates dCMP across from template dC with a frequency of 15-20%.

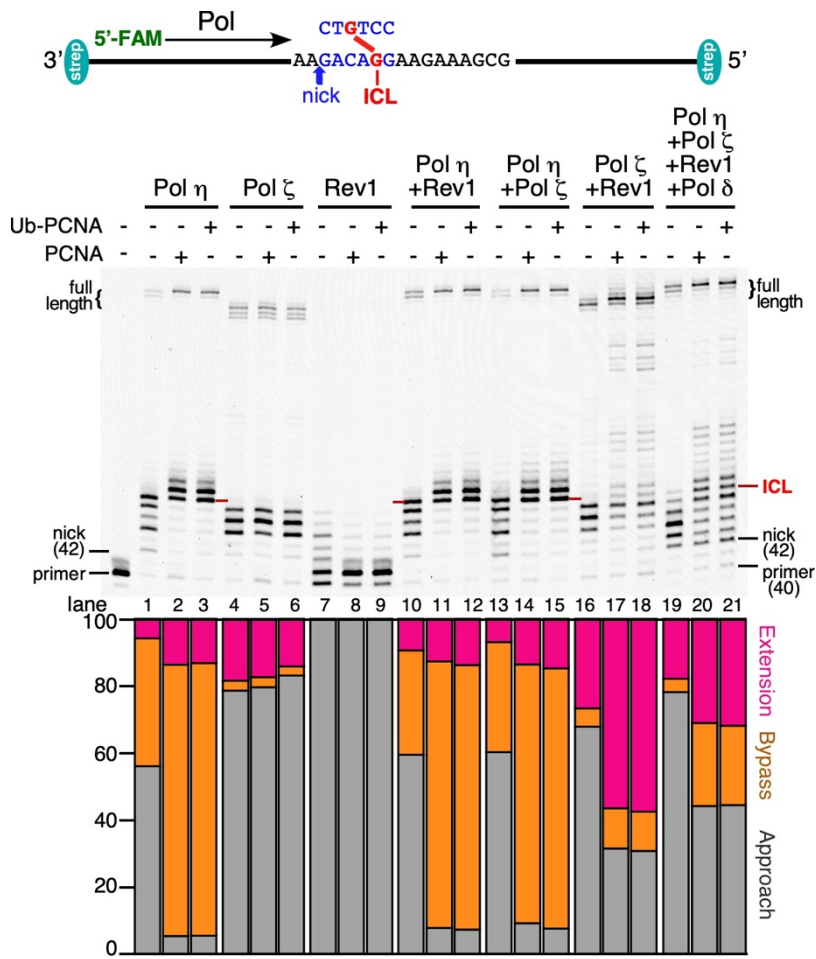


**Figure S5. Stimulation of ICL TLS by PCNA versus ubiquitinated PCNA.** Top, description of the substrate. Middle, the assay is as described in Figure 4, with either no PCNA, or 30 nM PCNA or ubiquitinated PCNA (as trimer), for 15 min at 30 °C. bottom, quantification of products in three classes.

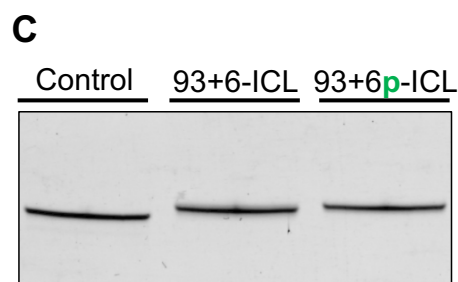
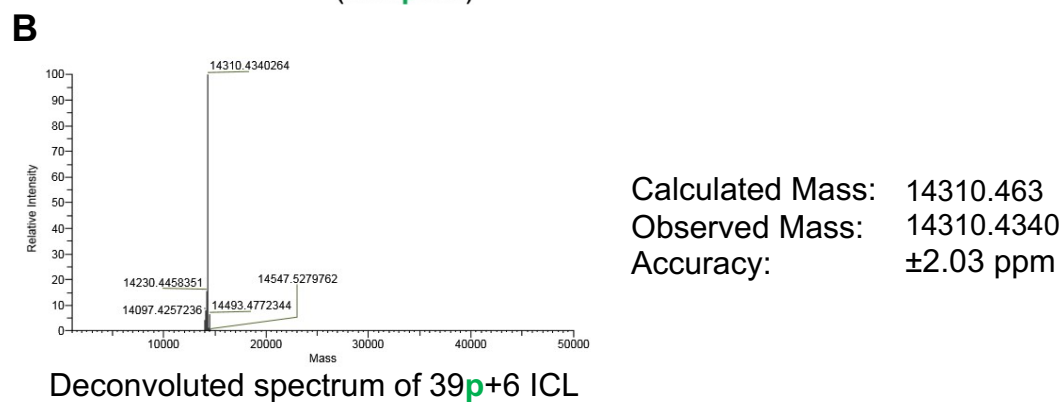
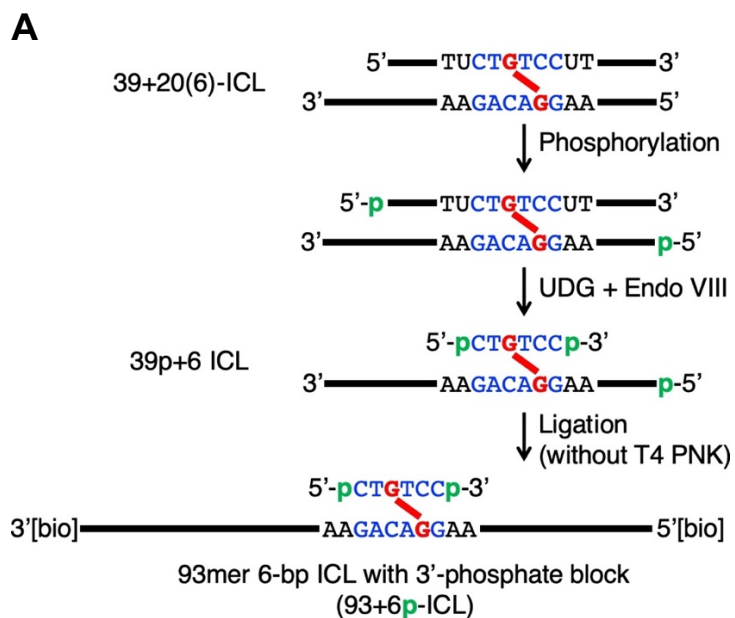


**Figure S6. Synthesis of ICL substrate with 3'-phosphate block. (A)** Synthesis scheme. **(B)** LC-MS analysis of 39mer intermediate. **(C)** 10% denaturing PAGE analysis of 93mer 6-bp ICL with 3'-phosphate block. "Control" refers to 93mer ssDNA. "93+6-ICL" refers to 93mer 6-bp ICL (**Figure 1A**).